Received: 16 August 2017 | Accepted: 23 August 2017
DOI: 10.1002/asna.201713403

ORIGINAL ARTICLE

Astronomische Nachrichten

# The variability of magnetic activity in solar-type stars

**D. Fabbian[1*] | R. Simoniello[2] | R. Collet[3] | S. Criscuoli[4] | H. Korhonen[5] | N. A. Krivova[1] | K. Oláh[6] | L. Jouve[7,8] | S. K. Solanki[1,9] | J. D. Alvarado-Gómez[10,11,12] | R. Booth[13] | R. A. García[14] | J. Lehtinen[1] | V. See[15,16]**

[1]Max Planck Institute for Solar System Research, Göttingen, Germany
[2]Geneva Observatory, Versoix, Switzerland
[3]Stellar Astrophysics Centre, Department of Physics and Astronomy, Aarhus University, Aarhus C, Denmark
[4]National Solar Observatory, Boulder, Colorado,
[5]Dark Cosmology Centre, Niels Bohr Institute, University of Copenhagen, Copenhagen Ø, Denmark
[6]Konkoly Observatory, Research Centre for Astronomy and Earth Sciences, Hungarian Academy of Sciences, Budapest, Hungary
[7]Université de Toulouse, UPS-OMP, Institut de Recherche en Astrophysique et Planétologie, Toulouse Cedex 4, France
[8]CNRS, Institut de Recherche en Astrophysique et Planétologie, Toulouse, France
[9]School of Space Research, Kyung Hee University, Gyeonggi, Korea
[10]European Southern Observatory, Garching bei München, Germany
[11]Universitäts-Sternwarte München, Ludwig-Maximilians-Universität, München, Germany
[12]Harvard-Smithsonian Center for Astrophysics, Cambridge, Massachusetts,
[13]Astrophysics Research Centre, School of Mathematics and Physics, Queen's University Belfast, Belfast, UK
[14]Laboratoire AIM, CEA/DRF-CNRS, IRFU/SAp, Centre de Saclay, Université Paris 7 Diderot, Gif-sur-Yvette, France
[15]School of Physics and Astronomy, University of St Andrews, Scotland, UK
[16]Department of Physics and Astronomy, University of Exeter, Exeter, UK

***Correspondence**
D. Fabbian, Max Planck Institute for Solar System Research, Justus-von-Liebig-Weg 3, 37077 Göttingen, Germany.
Email: fabbian@mps.mpg.de

**Funding Information**
German Federal Ministry for Education and Research. The Danish National Research Foundation, DNRF106. Hungarian National Research, Development and Innovation Office, OTKA K-109276. Chandra, AR4-15000X, GO5-16021X. Royal Astronomical Society. Science & Technology Facilities Council.

This article reviews the current knowledge and status of investigations on the variable magnetic activity of cool stars. We discuss the Sun in the context of solar-type stars, highlighting peculiarities and common features in terms of its magnetic activity and variability over different time scales. We examine how both theory and observations are providing new clues about the main physical processes that generate magnetic fields in the interior of cool stars, as well as about those that lead to evolving stellar surface magnetism and varying chromospheric and coronal phenomena. We then proceed to discuss the relations between stellar age, rotation, and activity throughout the evolution of cool stars. Finally, we touch upon the importance of understanding stellar magnetism also in view of its effect on planetary environments.

**KEYWORDS**
stars: activity – Sun: activity – stars: magnetic fields – Sun: magnetic fields

  

## 1 | INTRODUCTION

The Sun is currently a G2V-type star, having a photospheric effective temperature of ~5,770–5,780 K and living, like the majority of stars in the universe, through its main-sequence ("dwarf") phase. Because of the Sun's proximity to Earth, we know its physical conditions much better than those of other stars. Therefore, while among dwarf stars those of spectral type M (cooler, less massive, smaller, and dimmer than the Sun) are much more common, the solar case is used as a fundamental yardstick for astronomical studies.

Solar-type stars are main-sequence stars with a B–V color within ±25% that of the Sun (B–V ~ 0.65, see e.g., Bessell et al. 1998), and thus covering a range in spectral types from (the warmest among) K stars to (the coolest among) F stars. This definition fits approximately 10% of all stars. Despite this broad similarity to the Sun, their variability can be widely different in both amplitude and temporal scale. For example, the magnetic activity of these stars can manifest as multiple or single cycles in brightness variability, and the strength of the activity can vary across them. The cyclic behavior may even be interrupted by long quiescent periods (grand minima). It is important to relate this to the Sun's own variability and activity. In particular, many different observational diagnostics of the magnetic activity taking place on the solar surface can give a better insight into the still not fully understood Sun's internal dynamo. The comparison between different stars can then shed light on how stellar magnetism is generated and how it evolves with stellar age, and whether there exist different dynamo processes depending on the internal stellar structure.

The systematic search for stars with very similar properties to the (current) Sun, that is for solar analogs and solar twins (Cayrel de Strobel et al. 1981; Porto de Mello & da Silva 1997), started already several decades ago. Solar analogs are stars with a mass between 0.9 and 1.1 $M_\odot$, a surface chemical composition within 10% of the solar one, and similar effective temperature and photometric properties (e.g., bolometric luminosity) as the Sun. Solar twins obey even more stringent such requirements. Additionally, many of their other physical parameters (i.e., surface gravity, spectral type, color, radius, rotation, velocity fields, chromospheric activity, etc.) are virtually identical to the solar ones, so that these stars are spectroscopically indistinguishable from the Sun (e.g., do Nascimento et al. 2014, and references therein). They have an age within ±1.0 Gyr of that of the Sun (~4.6 Gyr), a time range during which they remain in a most stable state, with their magnetic activity level staying practically constant (in the case of the Sun, the ensuing variations in luminosity or total irradiance during its 11-year spot cycle are limited to one part in a thousand).

Studying solar analogs and solar twins allows us to understand whether the Sun is representative of nearby Sun-like stars. And, beyond the solar neighborhood, it provides important clues to test whether the Sun can truly serve as a reliable stellar evolution calibrator, or whether it instead is an outlier among stars of its age and mass. In the latter case, it is crucial, also for advancing the field of astrobiology, to clarify in which aspects the Sun may be exceptional, and whether its magnetic activity represents one of its peculiarities (e.g., Adibekyan et al. 2017; Kochukhov et al. 2017).

The cyclic activity of solar-type stars has traditionally (e.g., Durney et al. 1993; Spiegel & Weiss 1980) been ascribed to a dynamo mechanism maintained at the tachocline (the ~10-Mm-thick region at the base of the convection zone, separating the convective layers from the internal radiative zone). Rotational shear between the differentially rotating convective zone and the radiative zone, which rotates as a solid body, is thought to induce a large-scale magnetic flux that rises and emerges at the solar surface in the form of loops, heating the stellar chromosphere and corona.

Rotation in main-sequence solar-type stars slows down with time. As a result, the magnetic activity arising from the emergence of the magnetic flux generated at the tachocline decreases with age, too. The tachocline itself lies at increasing depths with later spectral types, disappearing at the boundary between early M and mid-M stars, more precisely around spectral type M3.5 (fully convective stars, see Reiners & Basri 2009). Thus, a direct comparison between the magnetic activity of solar-type stars and that of lower mass stars is essential to clarify the effect of stellar mass on the activity generated through a dynamo mechanism. The Sun, for example, likely experienced a significant increase in temperature and luminosity compared to when fusion of hydrogen nuclei into helium atoms in its interior first ignited. As other solar-type stars, during its main-sequence lifetime the Sun has also been spinning down as a result of magnetic braking, and the depth of its convection zone has been changing, both of which effects generate milder magnetic activity, with a great decline in the strength of magnetic heating, solar wind, and emission of high-energy particles.

The correlation between the rotational rate of a solar-type star and its chromospheric and coronal activity (e.g., emission in the Ca H & K lines, and in X-rays, respectively, see Basri 2016; Kraft 1967; Skumanich 1972) allows a rough estimation of its age. Observations of young solar analogs, in particular of their X-ray emission, provide a way to infer the conditions of the Sun back at the early times when it was much more active. Moreover, irradiation via energetic photons and particles is a likely key during the formation and evolution of planets (respectively, through star–disk interaction, i.e., the effect of the energy escaping from a pre-main-sequence star on its circumstellar disk, and through star–planet interaction, i.e., irradiation-induced changes in the properties of planetary atmospheres). Thus, studying the variable levels of magnetic activity of solar-type stars at all evolutionary stages is paramount for a clear picture of the environments in and around stars and planets (Güdel 2007).

Nowadays, space-based instrumentation, such as those onboard HINODE (Kosugi et al. 2007), SDO (Pesnell et al. 2012), and IRIS (De Pontieu et al. 2014), provides continuous monitoring of the Sun at sub-arcsecond spatial resolution over different spectral ranges. Such measurements complement multi-decadal full-disk observations of the photospheric and chromospheric magnetic flux (e.g., Ermolli et al. 2014, and references therein). Starting in 2019, the 4-m Daniel K. Inouye Solar Telescope (DKIST, see Tritschler et al. 2016) will observe the solar atmosphere at unprecedented spatial resolution and, by combining state-of-the-art instrumentation, will retrieve the solar magnetic field from the photosphere to the corona. Soon, the Solar Orbiter (Müller et al. 2013) will provide in situ measurements of the solar wind and imaging and spectropolarimetric observations of the solar surface (including the poles). Eventually, a next-generation space mission could even obtain solar data at ultrahigh spatial resolution at high temporal cadence (Collet et al. 2016). This constant progress in solar observations is complemented by a wealth of current and upcoming stellar spectroscopic/photometric data at increasing temporal resolution via surveys carried out on ground-based and spaceborne telescopes. Some of these scientific endeavors are *APOGEE* (e.g., Zasowski et al. 2013), *GALAH* (De Silva et al. 2015), *GAIA* (e.g., Mignard 2005), *4MOST* (de Jong et al. 2014), *PLATO* (Rauer et al. 2016), *TESS* (Ricker et al. 2015), and *JWST* (Greenhouse 2016). They will allow to us to perform unprecedentedly large statistical studies of stars in the Galaxy, which are set to greatly aid in disentangling its formation and evolution, as well as that of similar galaxies. These new data will also contribute to a better understanding of stellar physics, in particular of magnetic activity and variability throughout the lives of stars. Advances in various theoretical and computational aspects are very promising in this context, too. For example, three-dimensional radiation-(magneto)convection (3D R-(M)HD) simulations, proven to match observations better than one-dimensional static model atmospheres (e.g., Criscuoli & Uitenbroek 2014; Nordlund et al. 2009; Uitenbroek & Criscuoli 2011), have led to significantly revised solar composition estimates (Asplund et al. 2009; Fabbian & Moreno-Insertis 2015; Fabbian et al. 2010, 2012; Moore et al. 2016) and have been employed to retrieve stellar parameters from observations (Chiavassa et al. 2010; Collet et al. 2007), to study oscillations of Sun-like stars (Ball et al. 2016; Trampedach et al. 2017), to calibrate free parameters such as the mixing length in one-dimensional model atmospheres (e.g., Uitenbroek & Criscuoli, 2011), and to estimate the effects of surface magnetism on main-sequence stars (Beeck et al. 2015).

In this article, we offer a synthetic view of some recent advances and open questions in the domain of the variability of stellar magnetism, particularly in relation to the intimate interplay between magnetic activity and variability in Sun-like stars, and to the solar–stellar–planetary connection.

## 2 | SOLAR AND STELLAR VARIABILITY

The variability of the Sun and Sun-like stars has traditionally been investigated through the observation of solar and stellar chromospheres and coronae (Baliunas et al. 1995; Pizzolato et al. 2003), since the radiative output from these layers is considerably more variable and more simply related to the magnetic flux than that from the underlying photosphere (whose variations, manifested by starspots, have nonetheless been monitored using automated telescopes).

The variability of Sun-like stars is thought to be driven by a dynamo acting in the stellar interior. Total solar irradiance (TSI) is defined as the wavelength- and disk-integrated solar intensity—or in other words, the aggregate solar radiative flux or the power per unit area—as measured outside the terrestrial atmosphere and normalized to a distance of one astronomical unit. In recent times, thanks to very precise radiometers, the minute variability of TSI can be followed over entire solar cycles. Missions such as *CoRoT* (COnvection, ROtation and planetary Transits Baglin et al. 2006) and *Kepler* (Borucki et al. 2010), designed to look for faint planetary transits, have revealed the assorted variability of Sun-like stars in the visible spectral range. It is therefore timely to discuss solar and stellar variability, focusing on the bulk of the radiation, emitted mainly in the photosphere.

### 2.1 | Solar irradiance variability

The Sun has been known to be a variable star since 1978 when the first space measurements of TSI were carried out with sufficient accuracy to detect its small variations (typically one part in a thousand, e.g., Hickey et al. 1980; Willson & Hudson 1988). TSI has since been measured uninterruptedly, although with a changing array of instruments. It has been possible to merge these different datasets into a TSI composite, which shows that the Sun is variable at basically all time scales accessible to observations (Fröhlich 2003).

*Observed short-term variability*: The source of short-term solar variability depends on the time scale considered. With the exception of a range of periods around 5 min where solar p-mode oscillations display a set of discrete peaks, the contribution to solar variability for periods between minutes and multiple hours is dominated by granular convection at the solar surface (Harvey et al. 1985; Seleznyov et al. 2011). Because of the large number of granules present at any given time, the amplitude of this variability is generally small ($\approx$0.01%). On the time scale of solar rotation (about 27 days), variability is much higher (several tenths of percent) because of the combined effect of darkening induced by sunspots and brightening caused by faculae.

The most prominent cycle in solar irradiance variability is the 11-year cycle, coinciding with the sunspot periodicity of the Schwabe cycle. It is dominated by the network and facular contributions, which, against the sunspot contribution, cause a net TSI increase of only $\sim$0.1% at activity maximum. A further variability modulation of almost 2 years has been observed in different solar activity indicators (e.g., Berdyugina et al. 2002; Fletcher et al. 2010; Simoniello et al. 2013; Vecchio & Carbone 2009; Zaqarashvili et al. 2010). Its origin

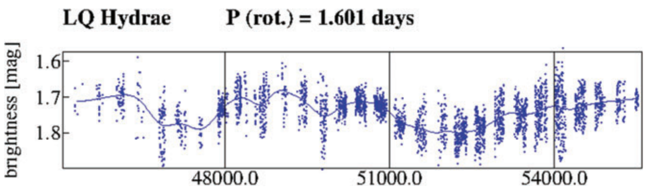


**FIGURE 1** Brightness evolution of the fast-rotating single K dwarf LQ Hya, based on 29 years (Julian date in abscissa) of photometric measurements. Figure adapted from Kővári & Oláh (2014)

is still debated but of great interest, as multiple magnetic cycles have been observed in other stars.

*Long-term variability*: The observational time series of solar irradiance are not long enough to investigate TSI variability at time scales spanning more than a few cycles with direct measurements. However, indirect indicators of solar magnetic activity show that the amplitude of the cycles varies with a period of 70–100 years. These roughly centennial variations can be inferred from sunspot number records (with time-resolved data on individual consecutive solar cycles), as first done by Gleissberg (1939), or on the basis of the effects of variable heliomagnetism on the production of isotopes in terrestrial, lunar, and meteoritic environments by cosmic rays (e.g., Knudsen et al. 2009; Usoskin 2013). These long-term solar activity indicators are complemented by another indirect proxy, that is geomagnetic activity data, especially useful to bridge the time period of significant anthropogenic disturbance of the $^{14}$C natural variability (and until satellite solar irradiance measurements became available). The open (or total) solar magnetic flux also shows a secular trend, for example a doubling during roughly 1900–1980 (Lockwood & Owens 2014; Lockwood et al. 1999) traced to overlapping cycles (Solanki et al. 2000, 2002).

Long-term photometric and Ca-index data for the Sun and active stars do hint (e.g., Oláh et al. 2009, 2016) that spot cycles are often multiple and that the periodicity of each cycle can vary. An example of complex cyclic (brightness) variations is given in Figure 1 for the active K2-type dwarf LQ Hya. Variations over a few years as well as on a decadal time scale are recovered, with the characteristic of the cycles apparently changing in time. The gray curve shows the spline-smoothed long-term variation.

Kolláth & Oláh (2009) (see also fig. 9 in Petrovay 2010) used sunspot and aurora records to infer the evolution of the Gleissberg cycle during the last 500 years, finding that its duration slowly increased from a length of ~50 years around 1750 to roughly a century or longer around 1950.

On still longer time scales, one sees large variations between the typical solar cycle amplitudes when comparing phases such as the modern Grand Maximum, a particularly long sequence of consistently strong (i.e., high-activity) cycles that the Sun seemingly experienced in the second half of the twentieth century (Usoskin 2017), to the almost sunspot-free period of the 1645–1715 Maunder Minimum (Inceoglu et al. 2016; Usoskin et al. 2015). The origin of these events is of particular interest to understand the mechanism(s) that cyclically regenerate solar and stellar magnetic fields.

*TSI reconstruction*: To assess the contribution of solar variability to changes in terrestrial climate, reconstructions of current and past TSI variations are needed. Most of these reconstructions are based on the observational evidence that TSI variations are induced by the evolution of surface magnetism. Although the available reconstructions differ in several aspects, such as the type of data employed to derive the evolution of the magnetic field (e.g., magnetograms, or photospheric and chromospheric imaging), the number and definition of magnetic structures contributing to the irradiance variations, and the models and techniques employed to estimate the radiative emission of magnetic features, most of them can reproduce ~90% of the observed TSI variations. Recent overviews of the solar-surface-magnetism-induced activity variability and of the available TSI reconstruction models are given in Domingo et al. (2009), Ermolli et al. (2013), Solanki et al. (2013), and Kopp (2016).

Reconstruction techniques have also been developed to attempt estimates of TSI variability at times prior to 1978. They return, additionally to cyclic variations, the secular trend in TSI, which is particularly important to constrain the contribution of solar irradiance to terrestrial climate. Whereas the reconstructions do not differ too strongly in the cycle variability, and give roughly the same temporal shape of the secular irradiance variations, they do not agree in the magnitude of the secular trend, with estimates of the increase between the Maunder Minimum and the modern Grand Maximum differing by a factor of 4–5 (e.g., Solanki et al. 2013), which translates into a change of the Earth global temperature of 0.08−0.3 K (Kopp et al. 2016). Such differences highlight our limited understanding of the magnitude and causes of long-term solar irradiance variability (the contribution of this stronger solar forcing to global surface-temperature increase is anyway significantly lower than the at least 0.8 K overall global warming known to have occurred over the same time frame). This should be borne in mind also when considering (and comparing with) longer term trends in the radiative flux of Sun-like stars.

The strength of spectral lines in the brightness spectrum on the Sun is known to change during the activity cycle since the pioneering Kitt Peak solar line-strength monitoring program (Livingston & Holweger 1982), followed later by many other investigations (e.g., Mitchell & Livingston 1991). An important development in solar irradiance modeling therefore has been the inclusion of spectral lines, with calculations (e.g., Unruh et al. 1999) showing that their varying contribution is the dominant factor producing TSI variations on solar-cycle time scales, while changes in the continuum level contribute negligibly. Further, spectral lines were recently found to play a very important role in determining the amplitude and the phase of TSI and solar spectral irradiance (SSI) variations at all time scales from the solar rotational period to centuries

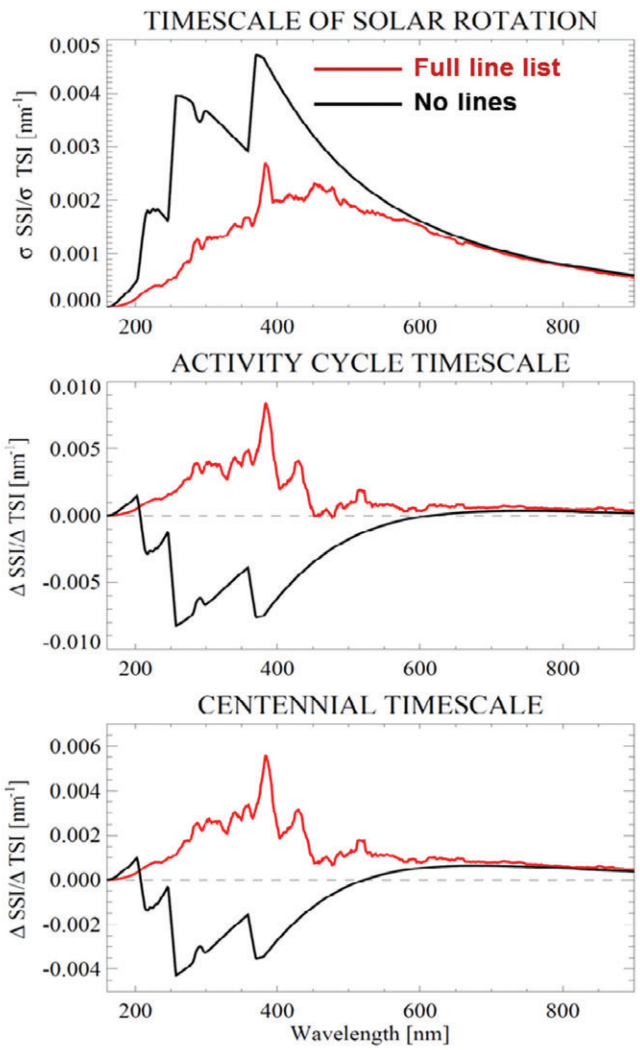


**FIGURE 2** Illustration of the influence of (atomic and molecular) spectral lines on solar irradiance variations. The spectral profiles of the rms irradiance variability calculated on the time scales of solar rotation (upper panel), of the solar activity cycle (middle panel), and of centuries (lower panel). The black curves are the result of pure continuum computations without any Fraunhofer lines, while the red curves are obtained by including both atomic and molecular lines with solar abundances (adapted from Shapiro et al. 2015)

(Shapiro et al. 2015), as illustrated in Figure 2. From it one can see that spectral lines lead to a reduction of the TSI variability in the ultraviolet and visible spectral ranges on the time scale of solar rotation, while on decadal (solar cycle) and centennial time scales the inclusion of spectral lines leads to a sign change of the variability (i.e., a 180° change in the phase of the respective cycles). Since the strength of the effect caused by spectral lines on irradiance variability obviously depends on the strength of the lines themselves (Livingston 1982; Livingston et al. 1977; Marchenko & DeLand 2014), this result has important implications for the variability of stars with different elemental abundances (stars with lower abundances having weaker lines) and effective temperatures (cooler stars having more and stronger spectral lines), see for example Yeo et al. (2016), and to test the solar–stellar analogy on the ground of variability.

## 2.2 | Stellar irradiance variability

Systematic observations of stellar variability have been carried out from the ground for over five decades (for even longer in the case of highly variable—and chromospherically/magnetically extremely active—stars, such as RS Canum Venaticorum and BY Draconis), beginning in March 1966 with Olin Wilson's initial measurements of the cores of the chromospheric Ca ii H&K lines in a set of 139 Sun-like stars. He carried out this effort, in his own words, "for the purpose of initiating a search for stellar analogues of the solar cycle" (Wilson 1968). Directly measuring magnetic fields in stars was not feasible at that time. Therefore, Wilson exploited the reversal to emission (first noticed by Eberhard & Schwarzschild 1913) that is present in the center of the broad Ca ii H&K absorption lines in the spectra of cool stars, and the fact that the strength of the emission in the cores of those lines had already for some time been used as a proxy for averaged magnetic field strength on the Sun. Wilson (1963) had already recognized a connection between stellar age and stellar activity after noticing that the intensity of the central emission in the lines of spectra of dwarf stars becomes weaker principally as a function of increasing age. He hypothesized this to be due to such stars starting their main-sequence lives with active chromospheres, which gradually become quieter as they evolve in time.

Soon after, Kraft (1967) found decreasing rotational velocities for increasing age in solar-type main-sequence stars. The picture connecting stellar magnetic activity to rotation via age was consolidated when Skumanich (1972) suggested that the braking effect could be expressed as a functional form that linearly relates the emission decay in the Ca ii H&K lines and the rotational decay to the inverse square root of the age. Skumanich thus predicted the proportionality between the strength of surface magnetic fields (known to be linearly related to the emission in those Ca spectral lines) and stellar angular velocity, due to the subsurface hydrogen convection present in dwarf stars of spectral type later than F5 likely giving rise to (magnetically active) chromospheres and significant winds. Such winds, as a result of the torque they exert in the presence of magnetic fields, are able to gradually decelerate the rotational rates of the star during all its evolutionary stages, even on the main sequence, thanks to the ensuing loss of angular momentum. This is well known as the crucial "rotation–activity(−age)" connection. It has its physical grounding in the fact that stellar magnetic dynamos depend on rotation and that angular momentum loss via stellar winds depends on the magnetic field (their coupling produces the magnetic braking effect) generated by the dynamo itself. As the star is being spun down, therefore, its dynamo-generated magnetic fields weaken and magnetic braking should gradually become milder (although field geometry should also play a role in controlling the strength of this rotational spin-down), see for example the recent review by Basri (2016).

The mentioned search (Wilson 1968) for stellar activity cycles finally brought to the realization that periodic, long-term chromospheric activity fluctuations over year-long time scales is encountered in many cool stars of different spectral types (Wilson 1978). Yet, some cool stars do not show any obvious activity variations, either because their magnetic activity is intrinsically constant in time, or because they may happen to be experiencing a solar Maunder Minimum-like state, or because the fluctuations themselves are below the current level of measurement precision or have longer periodicity than the time span covered by the observations. Irregular and multiple periodicity can also contribute to making a straightforward interpretation harder.

Modern ground-based observations include standard campaigns as well as data-gathering with automated telescopes. Additionally, several facilities have been running for decades gathering photometric data, for example the Vienna–Potsdam APT for about 25 years (e.g., Strassmeier et al. 1997), and spectroscopic data, for example STELLA for already more than a decade (Strassmeier et al. 2004).

With the help of comparisons with reference stars, it is possible to determine the variation in the Strömgren *b* and *y* bands over stellar activity cycles. Thus Lockwood et al. (1992, 2007) found that (a) the Sun has somewhat too low brightness variations for its activity level (compared to other stars in the observed sample), and (b) more active stars display an opposite dependence of irradiance on activity than the Sun. That is, instead of being brighter at activity maximum (as the Sun is), more active stars are darker. Regarding (a), Knaack et al. (2001) showed that the fact that we see the Sun in the equatorial plane, while other stars are seen at random inclinations, is not the explanation for the Sun's relatively low variability, as had been proposed by Schatten (1993). Regarding (b), Shapiro et al. (2014) used a simple extrapolation of the relationship between the coverage of the solar surface by faculae and plage areas to higher activity levels as a natural explanation of the opposite dependence of brightness on the activity level of more active stars.

The study of short-term (rotational time scale) variability in stars has taken a huge leap within the last decade. The *CoRoT* and *Kepler* missions have produced a vast library of light curves of Sun-like stars with a sensitivity that is starting to approach that of the solar radiometers. One of the many exciting results coming out of these datasets is that the short-term variability of Sun-like *Kepler* stars increases with decreasing rotational period (McQuillan et al. 2014; Reinhold et al. 2013; Walkowicz & Basri 2013). However, this is not universally accepted, as no dependence is found by García et al. (2014). Besides further observational studies, it is also urgent to understand such a possible dependence using a model that has proven itself for the Sun, where it can be well constrained thanks to the possibility of spatially resolving the solar surface. One idea is to use a flux-transport simulation (see Jiang et al. 2014, for an introduction to and overview of flux transport simulations) to evolve the surface coverage of spots and faculae on stars. This would be followed by calculations of the stellar radiative flux seen from a given vantage point at different rotational phases, following the technique of Dasi-Espuig et al. (2014, 2016). The idea is to change key parameters that are likely to influence the radiative output, such as the amount of magnetic flux in bipolar magnetic regions on the stellar surface, the locations of magnetic features on the stellar surface (both in latitude and longitude), and so on. The final step would be to compute synthetic *Kepler* observables with the aim of statistically reproducing the observations.

The accuracy of the *Kepler* data made it possible (Vida et al. 2014) to derive periodically changing photometric rotational periods on nine M dwarfs with periods shorter than 1 day. This may be caused by strong enough stellar surface differential rotation amplifying the smaller spot latitude changes over the (300–900 days) activity cycle for these fast-rotating stars compared to the Sun (butterfly diagram).

Recent observations of photometric variability in solar-type stars (Giampapa 2016) indicate that the transition between facular and spot dominance in brightness variations roughly coincides with the Vaughan & Preston (1980) gap in chromospheric activity (note that Marvin et al. 2016 recently extended from F to late M dwarfs the calibration of the absolute chromospheric flux emission). Nearly 80% of the single members in the sample analyzed are found to have no obvious periodicity. The only two among the non-binary stars with obvious periodicity appear to belong to the regime of reduced magnetic braking, that is their Rossby number (the ratio of the rotational period to the convective turnover time) is above a critical value. Chromospheric activity is enhanced with increasing stellar rotational velocity (i.e., with decreasing Rossby number); however, in the case of fast rotators it is crucial to exclude binarity by using radial velocity measurements at a precision better than 400 m/s. Studies of stellar rotational evolution should also include the impact of factors such as the presence of Jupiter-mass planetary companions in close-in orbits.

Generally speaking, the interplay between facular contrast, spot contrast, and fractional area coverage of surface features causes variations of stellar spectra, which depend on the particular wavelength and time scale being analyzed. Modeling of the main processes involved in the generation of magnetism in stars is therefore crucial in the interpretation of their photometric light curves. It is particularly interesting to investigate whether the bimodal evolution of stellar dynamos, as apparently implied by the existence of the Vaughan–Preston gap, that is by the relative absence of F and G stars of intermediate chromospheric activity levels, can be understood in terms of the Rossby number and/or of a rapid drop of the ratio of period of the cycle and period of the rotation for stars older than $\sim 2-3$ Gyr, in the sense of a switch between dynamo properties during their lives (Böhm-Vitense 2007; Hall 2008). This would include a change in patterns of differential rotation, meridional circulation, and a separation between surface-dominated shear in active stars (with spots providing the dominant contribution to variability) and tachocline-dominated shear (with variability dominated by faculae). Young, rapidly rotating, highly active stars with irregular and/or multipolar cycles would thus evolve into older, slowly rotating, low-activity stars with regular and/or dipolar cycles, with the current Sun possibly positioned in between these "Active" and "Inactive" branches. In fast-rotating stars, the Coriolis force is expected (e.g., Schuessler & Solanki 1992) to cause flux tubes to rise parallel to the axis of stellar rotation and emerge at high latitudes. Observations of rapidly rotating stars have, indeed, confirmed their tendency to manifest polar spots (e.g., Strassmeier et al. 1991; Vogt & Penrod 1983).

In the case of solar-type stars, the observed (flux) variability across the radiation spectrum (from X-rays all the way to radio wavelengths), caused by upward-rising magnetic structures within their atmospheres, can be interpreted by analogy with the Sun. The energetics that characterize different solar magnetic features can thus help explain the time evolution and amplitude of variability seen in various diagnostics for these stars. However, while observational data on stellar variability over up to decadal time scales are becoming increasingly available, little can be said about still longer term spectroscopic and photometric behavior of Sun-like stars (due to the limited temporal baselines of available measurements). Also, systematic monitoring of magnetic activity fluctuations in stars of different evolutionary stages is still scarce (e.g., Baliunas & Vaughan 1985).

## 3 | SOLAR AND STELLAR MAGNETISM

Stellar irradiance variability can be induced by different physical mechanisms. Among them, stellar pulsations (e.g., Chaplin et al. 2011a), granulation (e.g., Mathur et al. 2011), surface rotation (e.g., McQuillan et al. 2014), and magnetic activity (e.g., Mosser et al. 2009a) are some of those that, in general, affect main-sequence solar-type stars from high to low frequencies, respectively.

The Sun, because of its proximity, is the best studied star so far. Still, it is not clear whether it is peculiar in terms of its surface magnetism. To shed some light on solar magnetism compared to that of other Sun-like stars, it is paramount to study the photospheric and chromospheric activity levels of large sets of solar analogs. Moreover, the life of the Sun at previous times can be inferred by studying solar analogs and twins at different evolutionary stages (see e.g., Dorren & Guinan 1994). For this purpose, a high level of precision is required to characterize solar analogs in terms of age and other stellar parameters, but this is difficult when they are determined using classical methods.

### 3.1 | Magnetic activity in solar analogs

A segregation between an "Active branch" and an "Inactive branch" was first found by Saar & Baliunas (1992) when studying correlations of the normalised stellar cycle periods with the normalized dynamo numbers for a sample of carefully selected stars with well-determined cyclic periodicity. Brandenburg et al. (1998) later noticed that two different sequences appeared also when considering the behavior of the stellar activity cycle period as a function of the stellar rotational period. Böhm-Vitense (2007) further investigated the relationship between rotational periods and chromospheric activity cycle periods in Sun-like stars. The author found that the stars under investigation divided into at least two distinct sequences, with younger, faster rotating, more active stars clearly separated from older, slowly rotating, less active stars, and highlighted that some stars (on either branch) showed single magnetic activity cycles while others displayed double cycles. The existence of simultaneous but independent dynamo modes may, for example explain the presence of the Vaughan–Preston gap in chromospheric activity. Because of the convection zone layers moving increasingly deep with stellar age, they should experience stronger mixing and thus larger rotational velocity gradients. Fewer stellar rotations should then be necessary to wind up poloidal magnetic field lines and thus make the magnetic field strong enough that its toroidal component has sufficient buoyancy to rise to the surface, which possibly drives the creation of a secondary cycle in older stars.

The advent of ultrahigh precision space photometry from *CoRoT* and *Kepler* has started a new era in the study of solar-type stars, in particular of solar analogs, thanks to asteroseismology. For instance, the *Kepler* mission continuously monitored almost $2 \times 10^5$ stars during 4 years in the constellation of Cygnus and that of Lyra (Mathur et al. 2017). Using these observations, Chaplin et al. (2014) studied ~500 main-sequence and sub-giant, solar-type, pulsating stars from which Salabert et al. (2016a) identified 18 new solar analogs by combining asteroseismology with high-resolution spectroscopy. Four of these solar analogs turned out to be binaries (Salabert et al. 2016a). From the analysis of the individual mode frequencies, these stars have ages ranging from 1 to 8 Gyr (Metcalfe et al. 2014).

The photospheric magnetic activity index $S_{\rm ph}$ (García et al. 2010; Mathur et al. 2014)—calculated for 18 solar analogs found among *Kepler* stars and calibrated using the methods described by García et al. (2011)—is shown in Figure 3 (lower panel) as a function of the stellar surface rotation period obtained by García et al. 2014. Apart from the two youngest stars (KIC 5774694 and KIC 10644253, see Salabert et al. 2016a for further details), all other solar analogs are compatible with the photospheric (as well as chromospheric, see upper figure panel) activity levels of the Sun during cycle 23. They are thus analogs of the Sun also in this respect. However, it is important to keep in mind that (a) due to its dependency on the angle between the inclination axis of the star and the line of sight, $S_{\rm ph}$ is for low stellar inclination angles a lower limit of the actual photospheric magnetic field, and (b) this sample of solar analogs is selected based on asteroseismology,

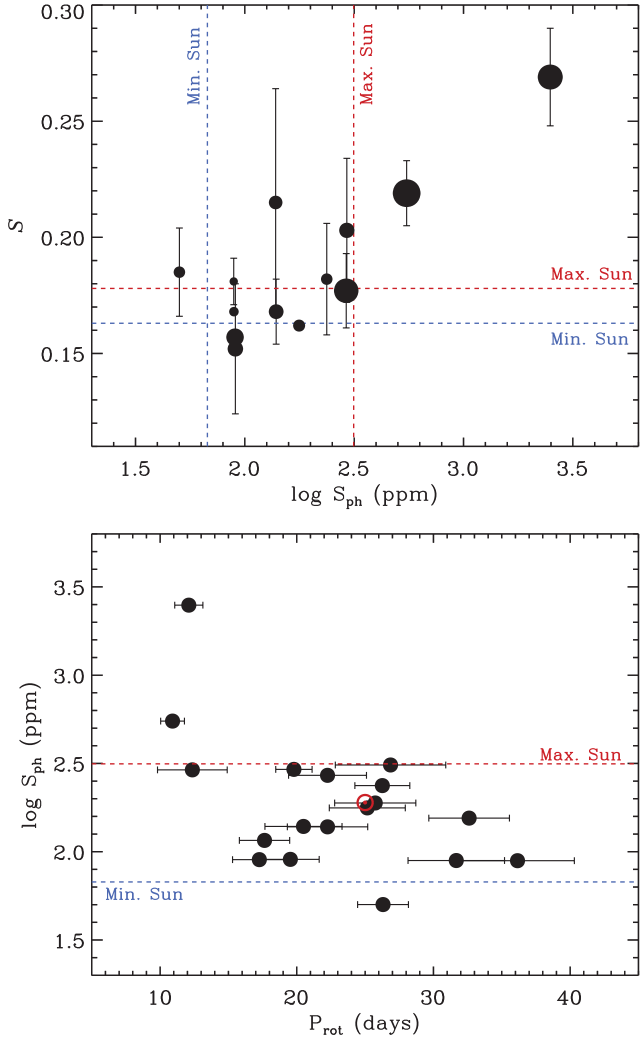


**FIGURE 3** Logarithm of the magnetic activity proxy $S_{ph}$ as function of the rotational period (lower panel) and of the chromospheric *S*-index as function of log $S_{ph}$ (upper panel). The dotted lines in both panels represent the photospheric and chromospheric magnetic activity levels for the Sun during the maximum (red) and minimum (blue) of cycle 23 (figure adapted from Salabert et al. 2016a)

and so it is biased toward relatively low photospheric magnetic activity levels, given that acoustic modes are inhibited by magnetic activity (Chaplin et al. 2011b; Jiménez et al. 2015; Mosser et al. 2009b; Simoniello et al. 2010).

The youngest solar analog in the sample, KIC 10644253, which shows a much higher activity level (and a more rapid surface rotation) than the Sun, was analyzed in detail by Salabert et al. (2016b). Its global properties as well as the length of its magnetic activity modulation are similar to the rapidly rotating young (active) solar analog HD 30495 studied by Egeland et al. (2015), who reported its short- and long-period variations. Salabert et al. (2016b) found that KIC 10644253 shows a correlation between the modulation in the p-mode frequencies and the magnetically induced modulation in activity observed as $S_{ph}$, with a ~1.5-Qyear period for both parameters. This short-period modulation could be similar to the solar quasi-biennial oscillation (see e.g., Fletcher et al. 2010; Simoniello et al. 2013).

## 3.2 | Constraining solar and stellar dynamo theory

The origin and evolution of magnetic activity in solar-type stars is ascribed to the dynamo process powered by the inductive action of the turbulent fluid in their interior. A consensus has been reached on the Ω-mechanism, thought to be able to generate a toroidal field by shearing a pre-existing poloidal field by differential rotation. Conversely, it is still a matter of debate which $\alpha$-effect regenerates the poloidal field from the toroidal one and where this mechanism takes place. There are two main possibilities: One is the $\alpha$ turbulent effect, which regenerates poloidal field by helical motion (Parker 1955; Steenbeck & Krause 1969). This mechanism may take place throughout the convection zone, or toward its bottom part, or in the interface layer called tachocline (e.g., Gilman & Miller 1981; MacGregor & Charbonneau 1997). Second is the Babcock–Leighton mechanism with the inclusion of meridional flow (Wang & Sheeley 1991).

Partially successful attempts have been made to even predict some characteristics of the solar cyclic behavior such as polar magnetic field reversals and the polar magnetic field strength at cycle minimum (e.g., Cameron & Schüssler 2007; Jiang et al. 2014; Upton & Hathaway 2014). Moreover, it is interesting to verify whether the dynamo mechanism might reproduce some of the observed features in solar-type stars. Yet another issue is that stars become fully convective at the cool end of the M-dwarf regime, for a spectral type of approximately M3.5. Late M dwarfs thus miss the interface region between the radiative core and the convective envelope, which was believed to be necessary for the generation of a dynamo (Parker 1985, 1993). As such, it is expected that these fully convective stars should not exhibit a rotation–activity relationship. However, recent evidence (Wright & Drake 2016) from observations of selected slowly rotating late M dwarfs seems to indicate that, in fact, even fully convective stars display a correlation between their X-ray emission and their rotational period similar to that present in solar-type stars. Since the X-ray activity–rotation relationship is a proxy for the magnetic dynamo behavior, these stars, too, are then likely to operate a solar-type dynamo mechanism. This would support the idea that the global magnetic field could originate throughout the convection zone (in the form of a distributed dynamo, see e.g., Brandenburg 2005), implying that the presence of a tachocline may not be crucial. In fact, dynamo mechanisms occurring in thin layers such as the tachocline should develop many toroidal field belts (Ruediger & Brandenburg 1995), which have never been observed.

Additional questions remain to be answered. For example, very recently Metcalfe et al. (2016) showed that the solar dynamo could be in a transition phase, implying that the Sun may be somewhat peculiar. de Jager et al. (2016) speculated that the fairly long period of low solar activity, which recently occurred between approximately 2005 and 2010, is an indication of a pulsating solar tachocline. Their hypothesis is that a relatively small (~0.03 solar radii) downward shift of the tachocline caused this recent phase, which would be a transition between the modern Grand Maximum and a forthcoming (likely regular) period of solar activity.

*Flux-transport dynamo models: applying the solar paradigm to stellar dynamos*. In order to model and understand the large-scale solar magnetism, a useful approach has been to make use of the mean-field dynamo theory (Krause & Raedler 1980; Moffatt 1978). This method has the advantage that it only deals with the large-scale magnetic field, assuming some parameterization of the underlying small-scale turbulence and magnetism. It is now appropriate to ask whether such mean-field dynamo models can be applied to other stars and whether they lead to good agreement with available observations. In particular, the observations seem to indicate that rapidly rotating solar-type stars tend to possess shorter magnetic cycles and to exhibit stronger toroidal field components. Simulations (e.g., Jouve et al. 2010) have been used in order to test whether the current dynamo models can reproduce such observations.

Among the various mean-field dynamo models, the Babcock–Leighton flux-transport dynamo models have recently been applied to the Sun. They successfully reproduced some solar observations, such as the 11-year cycle, the mid-latitude activity belt, the phase relationship between toroidal and poloidal fields or the equatorward propagation of sunspot emergence, and the degree of overlap during the activity minimum (see Charbonneau 2005; Simoniello et al. 2016). These models even start to be employed to tentatively predict some aspects of the next solar cycle using data assimilation techniques as commonly done in meteorology for decades (Dikpati & Anderson 2014; Hung et al. 2015).

In the Babcock–Leighton model, the toroidal magnetic field owes its origin to the differential rotation at play in the stellar convection zone, while the poloidal field originates from the decay of active regions after their formation at the stellar surface with a particular strength and tilt angle of the emerging magnetic field. If one then adds a large-scale meridional circulation, whose role is to advect the magnetic field concentrations inside the convection zone, the model is called a flux-transport model. These flux-transport models are able to produce a magnetic field regularly reversing its polarity. The cycle period is found to be sensitive to the meridional flow amplitude $v_0$. Dikpati & Charbonneau (1999) and Jouve & Brun (2007) report scalings such as $P_{\rm cyc} \propto v_0^{-0.83}$. However, even for the Sun, the characteristics of the meridional flow (deduced via helioseismology) are poorly constrained (see review by Gizon et al. 2010).

Jouve et al. (2010) found that the magnetic cycle period in Babcock–Leighton flux-transport dynamo models with faster rotation and thus slower meridional circulation is much longer than suggested by observations. While it is possible to reconcile the discrepancy by reducing the dependency of the magnetic cycle period on $v_0$, for example by invoking other transport processes such as turbulent diffusion or magnetic pumping (Do Cao & Brun 2011; Guerrero & de Gouveia Dal Pino 2008; Hazra et al. 2014), a well-calibrated model for the Sun needs severe modifications to fit stellar observations. In fact, since Babcock–Leighton models are based on our knowledge of the Sun's flow field and still require free parameters, they likely can reproduce any result within the large uncertainties on stellar flows.

*3D MHD global convective dynamo models*: Another approach to understand the generation of the large-scale magnetic field is to solve the full set of magnetohydrodynamical (MHD) equations, allowing to self-consistently to produce the flow and magnetic field structures that will interact nonlinearly. The past few decades have seen the advent of multidimensional numerical simulations to model the intricate evolution of the solar magnetic field.

In the case of 3D MHD global dynamo models, the MHD equations are solved in spherical geometry. The necessary calculations are thus obviously much more costly than for 2D mean-field dynamo models but have the decisive advantage of self-consistently computing the flows and magnetic fields. Tremendous progress has been made in the past decade on simulations of 3D MHD global dynamo models, and several properties about stellar convection, large-scale flows, and dynamos have been found to be quite robust (see review in Brun et al. 2015). For instance, these models all show that the profile of differential rotation is directly linked to the Rossby number of the simulation, which is a measure of the importance of the inertia term compared to the Coriolis term in the Navier–Stokes equation. Indeed, it was found by several authors that anti-solar differential rotation (slow equator, fast poles) occurs at large Rossby numbers, whereas Sun-like differential rotation (fast equator, slow poles) occurs at small Rossby numbers (e.g., Gastine et al. 2014). In the absence of conclusive detection of meridional circulation in stars other than the Sun, 3D MHD global dynamo calculations predict a tendency for it to become more and more multicellular (with several circulation cells appearing both in latitude and radius (Featherstone & Miesch 2015) for rapidly rotating models (i.e., those characterized by small Rossby numbers), and that its amplitude should decrease with increasing rotational rate (Augustson et al. 2012; Ballot et al. 2007; Brown et al. 2008) with a typical scaling such that $v_0 \propto \Omega_0^{-0.45}$. On the observational side, nevertheless, no existing evidence supports the possibility of anti-solar differential rotation in cool stars with large Rossby numbers (weak rotational influence). Moreover, the inability of the 3D MHD global models to reproduce the differential rotation of the Sun for solar rotational rate and energy flux remains a serious issue. On the other hand, the large-scale hydrodynamic theory of differential rotation in convection zones based on the turbulence-induced lambda-effect seems to reproduce the observations for cool stars (including the data from the *MOST* and *Kepler* missions) very well (Rüdiger et al. 2013).

Concerning magnetic fields in 3D MHD global dynamo models, various types of behavior have been recovered, in particular widely different underlying dynamo action, that is from steady to irregular to well-defined cyclic magnetic activity. For low-mass stars (spectral type M), numerical simulations tend to demonstrate the ordering role of the Coriolis force, also seen in planetary dynamos (Christensen & Aubert 2006). More specifically, when the Rossby number is increased, the magnetic field switches from mostly dipolar to mostly multipolar. However, it has also been found that the low Rossby number regime could maintain both a dipolar and a multipolar solution depending on the initial magnetic conditions. This interesting bistability was also seen in observations (Morin et al. 2010) showing that stars with very similar rotational rates and masses (thus probably similar Rossby numbers) may exhibit very different magnetic fields (strong and dipolar vs. weak and multipolar). In simulations with stronger stratification, this bistable behavior seems to disappear. More computations are needed to further investigate this. For instance, a recent simulation of a fully convective star by Yadav et al. (2015) with a reasonable degree of stratification (a density ratio of 150) was shown to possess both large-scale (mostly dipolar) and small-scale magnetic fields. A Zeeman–Doppler imaging (ZDI, see Sections 4.3 and 5.2) reconstruction was then applied to the simulation to see how well this analysis technique was able to recover the magnetic field content. As expected, the large-scale strong polar spot was perfectly recovered but not the smaller-scale features, which represent most of the magnetic flux in the simulation.

Simulations of solar-type stars with high rotational rates have also been performed, showing strong belts of toroidal field in the convection zone which can undergo cyclic reversals as the level of turbulence is increased (Brown et al. 2011; Käpylä et al. 2013; Nelson et al. 2013). Some Maunder Minimum-like periods were even found in some simulations of F stars (Augustson et al. 2013). It is still not entirely clear what sets the periodicity in the models that develop cyclic reversals. From the published results, the meridional circulation amplitude does not seem to play a key role in establishing the time scale for the magnetic cycle, contrary to what is assumed in a Babcock–Leighton flux-transport dynamo model. Moreover, simulations of 3D MHD global stellar dynamos are not able to produce spots at the surface of the models (owing, presumably, to the fact that they lack the sufficient resolution) and may thus be difficult to reconcile with Babcock–Leighton models. However, with the help of Doppler imaging, poleward flow patterns, which are possibly the outer manifestation of meridional circulation (as supported by theoretical expectations of magnetically induced thermal inhomogeneities, see Kitchatinov & Rüdiger 2004), were observed on the surface of the active giant sigma Gem (Kővári et al. 2015).

Most of the simulations cited above do not possess a tachocline and a stable layer beneath. Only recently have some simulations been performed with a tachocline and comparisons with convective shells with similar properties start to be done (Guerrero et al. 2016). It is reported that a tachocline helps to organize the magnetic field by building strong concentrations of large-scale field, but the influence on the cyclic behavior of the solution needs to be clarified.

*Flux emergence: what properties of solar flux emergence could be applied to other stars*? In Babcock–Leighton dynamo models, the process of magnetic flux emergence through the stellar convection zone is crucial since the source of poloidal field is directly linked to the presence of active regions. In 3D MHD global dynamo models, the strong toroidal structures developed in rapidly rotating stars can become buoyant (Fan & Fang 2014; Nelson et al. 2014) but rarely rise all the way to the top of the computational domain. Consequently, those models do not produce spots. It is thus still an open question whether one can really rely on spotless dynamo models to reproduce the magnetism of stars, and in particular of the Sun. In the case of 3D MHD, only fully compressible local simulations are able to model flux emergence near the solar surface, while global simulations of convective dynamo action are able to generate buoyant magnetic loops in a Sun-like stellar model but their resolution is insufficient to model granulation and supergranulation and thus the emergence of magnetic flux at near-surface layers (Nelson et al. 2014).

Because magnetic flux emergence is very important for Babcock–Leighton dynamo models, detailed numerical simulations of the flux emergence process in the Sun (e.g., Cheung & Isobe 2014; Martínez-Sykora et al. 2008; Yelles Chaouche et al. 2009) are potentially of considerable importance also for understanding the dynamo mechanism. It has to be noted that other theories exist that do not rely so heavily on the presence of strong toroidal structures built in the tachocline and then becoming unstable. Some authors (Brandenburg et al. 2013; Stein & Nordlund 2012) have argued that local flux concentrations by convective motions or by instabilities appearing in very strongly stratified zones could also lead to the formation of active regions in the Sun. We will here concentrate only on the first picture of flux tubes rising from the base of the convection zone where they are produced to the surface where they emerge as spots.

As mentioned, numerous numerical simulations of solar flux emergence have been performed (see review in Fan 2004), to compare with the detailed observations of active region formation and evolution in the Sun. An illustration of a numerical simulation (Jouve et al. 2013) of a buoyant loop rising in a convective shell is shown in Figure 4. However, very few investigations have been conducted on similar processes of flux emergence in other stars. Thin flux tube calculations exist for giants (Holzwarth & Schüssler 2001) and rapidly rotating stars (Holzwarth et al. 2006). Simulations of thin flux tubes evolving in a fully convective star have recently been performed by Weber & Browning (2016).

Nowadays, many indications exist of spots on other stars, with various degrees of stellar surface coverage and magnetic fluxes. These properties have strong implications for potential eruptive activity on those stars and consequences on the surrounding planets. Some properties found in simulations of

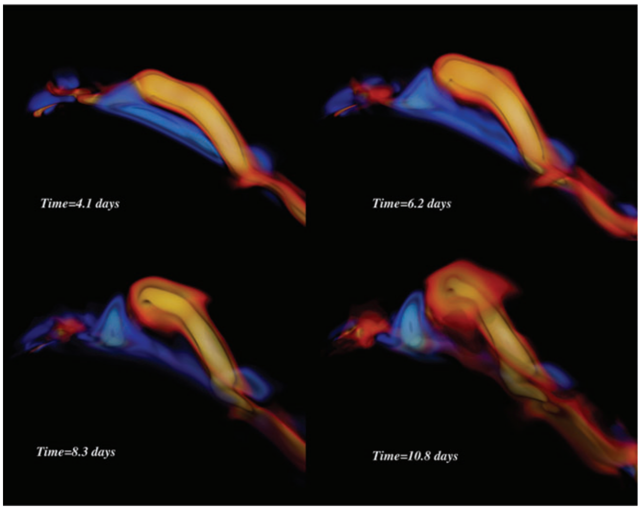


**FIGURE 4** Volume rendering of the toroidal magnetic field of a loop rising through a convective layer

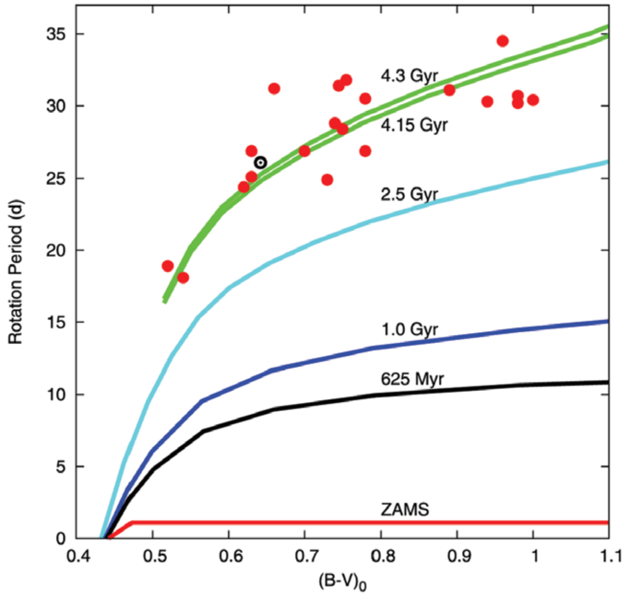


**FIGURE 5** M67 color–period diagram. Rotational isochrones are overplotted for different ages, as marked, including for 4.15 and 4.3 Gyr (mean and median cluster age, respectively). The current Sun is ∼1$\sigma$ above the latter two curves, while the dominant source of scatter around them of the M67 FGK stars is observational. See Barnes et al. (2016) for further details

large-scale flux emergence in the Sun could easily be applied to other stars. In particular, the rise trajectory of field concentrations from the base of the convection zone to the surface is strongly influenced by the Coriolis force, with a tendency of flux tubes in a fast rotating environment to rise parallel to the axis of stellar rotation and thus emerge at high latitudes. One may thus expect rapidly rotating stars to exhibit spots at high latitude, a hypothesis that seems to be in reasonable agreement with observations. The typical size of active regions is then another question that could be addressed through numerical simulations of flux emergence in a convective domain. It remains to be understood in detail whether this size is determined by the mean size of convective cells (which is different in stars rotating at significantly different rates) or by the typical length scale of the buoyancy instability.

## 4 | VARIABILITY OF MAGNETIC ACTIVITY THROUGHOUT STELLAR EVOLUTION: OBSERVATIONS AND THEORY

In this section, we touch upon the topic of activity variability for cool stars with different rotational rates and ages, as retrieved from surveys and inferred by theory. The complex physical interaction between rotation, convection, magnetic fields, and winds in main-sequence stars of different evolutionary stages is the key to understanding their variability.

Variability in coronal X-ray emission, Ca ii, or H$\alpha$ emission (West et al. 2008) is thought to be driven by the stellar magnetic dynamo. Emission in these chromospheric and coronal magnetic activity tracers is found to decrease monotonically with decreasing rotational velocity (Pallavicini et al. 1981), or in other words with increasing stellar age. This is attributed to the rotational spin-down due to mass loss through a magnetized stellar wind (e.g., Skumanich 1972). Such wind is also believed to be driven by the stellar dynamo (Cranmer & Saar 2011), so that rotation and magnetic activity effectively operate in a feedback loop, and rotation, stellar activity, and stellar wind will all decrease with age. Thus, the investigation of solar/stellar activity proxies is a probe of the dynamo process throughout stellar evolution and can also be used to infer the age of a given star.

A different method called "gyrochronology" is also used to derive ages for low-mass, main-sequence stars. The method employs only two observables: rotational periods and colors, and was tested on coeval stars in clusters by Barnes (2007, 2010) and Barnes et al. (2016). M67 has been observed by *Kepler*'s *K2* mission providing excellent rotational periods of FGK stars in the cluster. Figure 5 shows that the position of the Sun (black circle) on the color–rotational period diagram agrees very well with the rotational isochrones (green curves) of FGK rotators (red filled circles) of M67, which is found to be ~4.2 Gyr old (for further details, see Barnes et al., 2016a, 2016b). Applying the method to the full (36-year-long) S-index dataset of field solar-type stars by Wilson (1968), the activity–age dependence of 28 solar-type stars was established by Oláh et al. (2016), see Figure 6. The age behavior of those stars shows a bimodal distribution of cycle lengths and types (simple vs. complicated cycles). The separation between the two modes of the distribution occurs at the age of ~2.2 Gyr, that is at the Vaughan–Preston gap, when the higher and lower level of activity of the stars (cf. active and inactive branches) suggest that the underlying dynamo is undergoing a change.

### 4.1 | The stellar age–activity relationship beyond a Gigayear

The age–activity relationship uses the change in stellar magnetic activity over time to infer the ages of stars. This

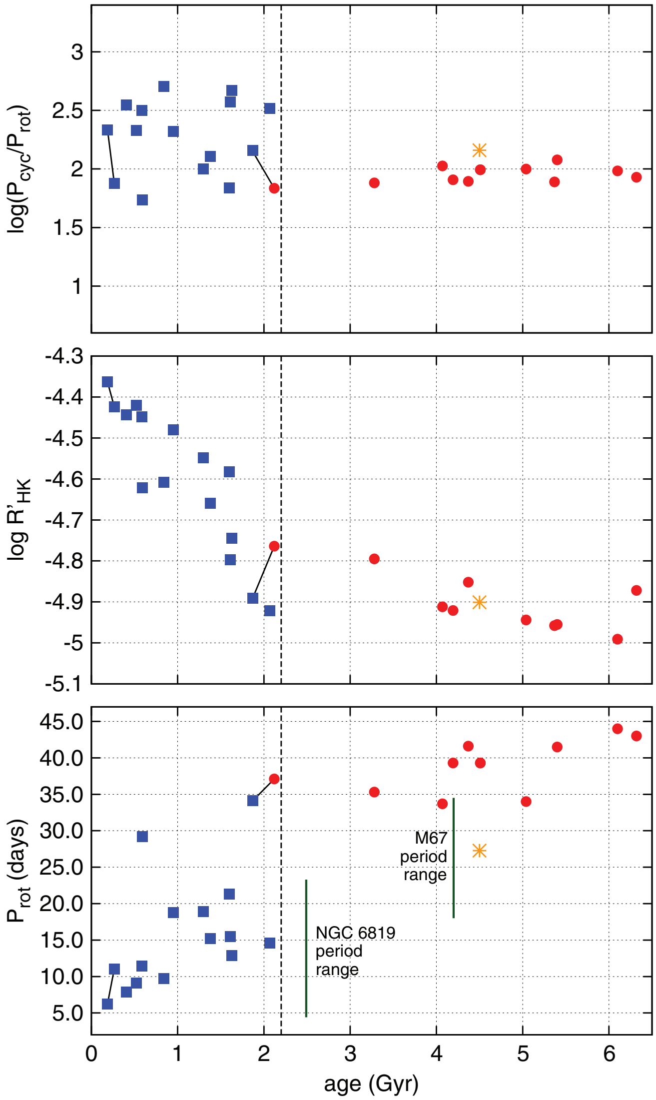


**FIGURE 6** (From lower to upper panel) Rotational periods, logarithm of the activity indices, and logarithm of the cycle periods normalized with the rotational periods, as a function of the gyrochonologically derived age of solar-type stars, using the calcium index datasets from the Mt. Wilson survey. Wide binaries are connected with lines: the apparent age difference between the (coeval) components indicates the scatter in the determination of age from rotation. See Oláh et al. (2016) for further details

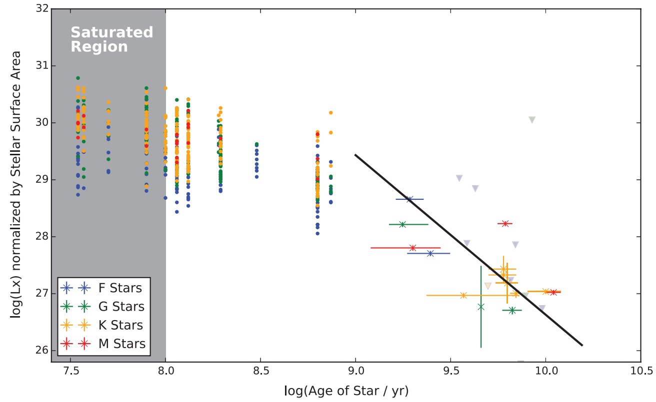


**FIGURE 7** A log–log plot of normalized X-ray luminosity as a function of stellar age. Filled circles mark the X-ray luminosities measured for stars in a given cluster (data from Jackson et al. 2012). Data points with error bars show the stars analyzed by Booth et al. (2017). Upper limit results are denoted by downward triangles in gray color. The black line indicates the best fitting age–activity relationship found for the data analyzed by Booth et al. (2017)

change in activity is a result of decreased rotational velocity (a consequence of magnetic braking) causing reduced magnetic field generation by the stellar dynamo. For a discussion on how the evolution of stellar rotation can be understood as a function of stellar radius, see Reiners & Mohanty (2012). Therefore, by studying the age–activity relationship one can gain insight into how the stellar dynamo evolves over time.

This relationship requires calibrator stars whose ages have been determined via other methods. Currently, the employed stars are younger than a gigayear. However, asteroseismology has become a valuable tool in determining the ages of solar- and late-type stars, providing suitable calibrator stars. Booth & Poppenhaeger (2016) used ages from recent asteroseismology studies coupled to the X-ray luminosities (used as stellar activity proxy) to investigate the age–activity relationship for stars older than a gigayear. They modeled the observational spectra with a coronal plasma model. From the best fitting model, the X-ray flux was calculated in the 0.2–2.0 keV energy range, as this is typically where the spectra of solar- and late-type stars peak in the X-ray range. For X-ray sources not detected to a sufficient confidence level, upper limits to the X-ray fluxes were determined. Combining their flux with their distance, they calculated the X-ray luminosity of each star.

A previous study by Jackson et al. (2012) investigated the age–activity relationship by using clusters as calibrators (since stars in a given cluster share the same well-determined age). They found that for very young stars there is a saturation of the X-ray luminosity. The X-ray saturation ends at ~100 Myr, when the luminosity starts to decay. In the unsaturated region the X-ray luminosity decreases with a gradient of ~1.2 (depending on spectral type). Figure 7 shows the results of Booth et al. (2017) alongside the cluster data from Jackson et al. (2012). The X-ray luminosity beyond 1 Gyr is seen to decrease with age, as expected. However, the best fitting relationship for these older stars has a gradient of $-2.80 \pm 0.72$, which is steeper than the gradient found for the cluster data.

A theoretical age–activity relationship can be derived by considering two relationships. The rotational velocity of a star will decrease over time as a result of magnetic breaking where the rotation is related to the age by $v_{rot} \propto t^{-\alpha}$ where $\alpha = 0.5$ (Meibom et al. 2011; Skumanich 1972). Observations of solar-type stars confirmed that the relationship between activity and rotation takes the form $L_x \propto v_{rot}^{\beta}$ where $\beta = 2$ (Pizzolato et al. 2003). From these two relationships one can predict how X-ray luminosity varies with time via the following equation: $L_x \propto t^{-\alpha\beta}$ where $\alpha\beta = 1$.

One possible explanation for the larger value of $\alpha\beta$ found by Booth et al. (2017) compared to the theoretical value is that the rotational spin-down for stars older than a gigayear may be more rapid than expected from constant magnetized stellar winds (Kawaler 1988). However, a recent study by van Saders et al. (2016) provides evidence of weakened magnetic breaking for older late-type stars. Other theoretical work (e.g., Garraffo et al. 2015; Vidotto et al. 2016) shows that the rotational spin-down of a star may depend on the magnetic field geometry. If the change in rotational spin-down was the only factor affecting the change in the age–activity relationship, then one would expect to see evidence of weakened magnetic braking, resulting in a decrease in the value of the exponent of the age–activity relationship. Instead, the increased value of the exponent found by Booth et al. (2017) suggests that another mechanism is causing the change in the age–activity relationship.

The other possible explanation for the increased decay in magnetic activity for stars older than a gigayear is that the relationship between the X-ray luminosity and rotational velocity is not constant. There is some evidence for the steepening of the activity–rotation relationship. Wright et al. (2011) considered a small, unbiased subset of their large sample of solar and late-type stars and found that a value for $\beta$ of 2.7 was a better fit for their data than the generally accepted value of 2. One of the lowest X-ray luminosity values considered in the Wright et al. (2011) subset of data was the solar one, while the study by Booth et al. (2017) included older stars, which have lower X-ray luminosities than the Sun. More research is still needed into the activity–rotation relationship to confirm its steepening toward old stellar ages. Future combined studies of age, rotation, and activity will be able to shed light on which components of the relationship are responsible for this.

## 4.2 | Rotation and spot activity of young solar-type stars

With their fast rotational rates, young solar-type stars have notably higher activity levels and somewhat different activity behavior than the Sun, despite being otherwise physically comparable objects. These differences in activity offer a valuable window into the working of stellar dynamos at different physical parameter ranges and shed light on the evolution of the activity of the Sun since its birth.

Both young and old solar-type stars commonly show signs of activity cycles in their chromospheric emission (Baliunas et al. 1995) as well as in broadband photometry (Oláh et al. 2009), whenever long enough time series of observations are available. In photometry, the varying mean brightness of the active stars corresponds to the changing levels of spottedness that the active stars undergo. When the periods of these chromospheric and spot (i.e., stellar activity) cycles are compared with the stellar rotational rates or activity levels, they cluster on a sequence of activity branches (e.g., Brandenburg et al. 1998), conventionally called the “Inactive”, “Active”, and “Superactive” branches.

The cycles of the young, fast-rotating stars are found along the junction between the “Active”, and “Superactive” branches, see Figure 8. In it, we compare the spot cycles of the young (<0.6 Gyr) solar-type stars studied by Lehtinen et al. (2016) with the cycles of a broader stellar sample from Saar & Brandenburg (1999). The figure shows the dependency between the logarithm of the ratio of period of rotation ($P_{\rm rot}$) to period of the cycle ($P_{\rm cyc}$) and the chromospheric emission index $\log R'_{\rm HK}$ of the stars, revealing a clear picture of the activity branches, equivalent to what seen when using the inverse Rossby number instead of $\log R'_{\rm HK}$.

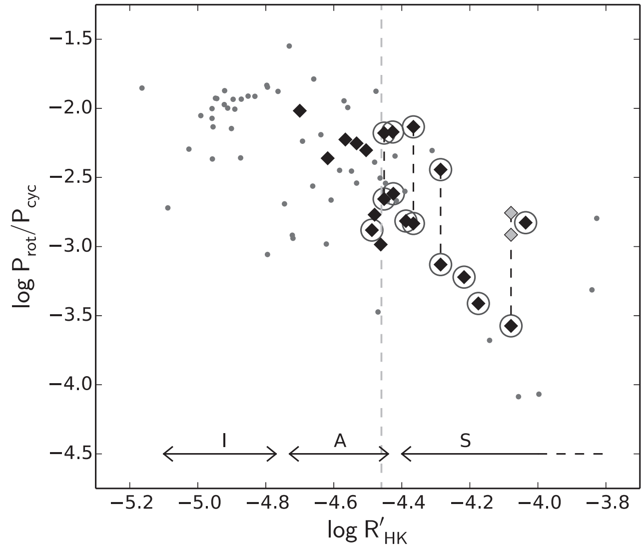


**FIGURE 8** Logarithm of the ratio between the rotational period and the cycle period as function of the chromospheric activity index for stars from Lehtinen et al. (2016, black diamonds) and Saar & Brandenburg (1999, small gray dots). Additional short cycles from Oláh et al. (2009) are shown for LQ Hya (gray diamonds). Stars with observed active longitudes have their symbols circled. The transition between stars with axisymmetric and non-axisymmetric spot distributions is shown by the vertical dashed line. The approximate ranges of the “Inactive”, “Active”, and “Superactive” branches are shown with the arrows labeled “I”, “A”, and “S”

The young stellar sample clearly shows that the younger stars have fractionally longer cycle periods (cf. Oláh et al. 2016) and that the “Superactive” branch has an opposite slope to what the “Active” and “Inactive” branches are understood to have (Saar & Brandenburg 1999). In fact, the sample seems to include the turnoff point between the “Active” and “Superactive” branches. More strikingly, the “Superactive” branch appears now split into two parallel sub-branches that have a cycle period ratio of roughly $P_{\rm cyc,1}/P_{\rm cyc,2} \approx 5$ between them. These sub-branches seem quite robust, since each star in the sample with two cycles of different lengths have their cycles tightly on the opposite sub-branches. Additional short-cycle period estimates for the very active young star LQ Hya by Oláh et al. (2009) also conform to this picture by falling tightly on the opposite sub-branch than the long cycle period reported for the star by Lehtinen et al. (2016). It seems probable that the sub-branches correspond to two different cycle modes that can be simultaneously excited in the stellar dynamos.

Another common feature of the spot activity observed on young active stars are the strong and well-developed active longitudes. These are structures where the spot activity of a star is confined to one or two narrow longitudes that can stay intact for more than a decade, far longer than would be expected for active regions eventually broken down by differential rotation. Not all active stars have active longitudes: Lehtinen et al. (2016) observed that only the faster rotating and thus more active stars show evidence for their presence. There appears to be a quite sharp boundary at around $\log R'_{\mathrm{HK}} = -4.46$ between these stars and the stars where the long-term spot distribution is axisymmetric. This is expected both in the light of mean-field dynamo theory (Krause & Raedler 1980) and modern direct numerical dynamo simulations (Käpylä et al. 2013) that predict the development of non-axisymmetric dynamo modes on stars with low Rossby numbers. Still further evidence for the development of non-axisymmetricity on fast rotators was provided by See et al. (2016) who found that $Ro \approx 1$ defines an approximate limit that confines stars with non-axisymmetric, large-scale magnetic fields mostly on its lower side.

The active longitudes do not necessarily follow exactly the bulk rotation of the star. A number of the stars in the sample of Lehtinen et al. (2016) show prograde migration of their active longitudes with respect to the mean stellar rotation. The same phenomenon has also been observed on the superactive binary II Peg (Hackman et al. 2011; Lindborg et al. 2011), where it was possible to compare accurately the active longitude rotation with the orbitally synchronized bulk rotation of the star. It is, in principle, possible to explain this phenomenon as a signature of radial differential rotation if we consider that the spot-generating structure of the active longitudes is anchored at a different depth in the stellar interior than the individual decaying spots. However, such active longitude migration patterns are again predicted by the dynamo theory. In the mean-field dynamo solutions the non-axisymmetric dynamo modes generally exhibit some sort of migration in the form of a very slow, retrograde azimuthal drift in the stellar rotational frame of reference (Raedler 1986) and this same migration is also present in direct numerical simulations (Cole et al. 2014) as an azimuthal dynamo wave. Nevertheless, the exact relation between the observed active longitude migration patterns and dynamo theory remains an open problem, in particular the discrepancy between the predicted retrograde migration and observations of prograde migration of the active longitudes.

### 4.3 | Stellar activity cycles from Zeeman–Doppler imaging

As already discussed, it has long been known that stars possess activity cycles, as, for example manifested by their tendency, when exploring the dependency of the period of their activity cycle on various stellar parameters, to cluster along separate branches, and by the periodic variations in Ca ii H & K emission on yearly to decadal time scales.

ZDI is a tomographic technique that can be used to reconstruct the large-scale magnetic field geometry at the surface of cool stars (Donati & Landstreet 2009). Over the last decade, various ZDI studies have been conducted to determine how field properties vary as a function of fundamental stellar parameters (Folsom et al. 2016; Morin et al. 2010; See et al. 2015; Vidotto et al. 2014). We now briefly analyze the magnetic properties of stars on the active and inactive branches. Böhm-Vitense (2007) suggested that the dominant shear layer for dynamo action in inactive branch stars is the tachocline, while for active branch stars it is the near-surface shear layer.

Figure 9a shows the cycle period versus rotational period for the sample studied by Böhm-Vitense (2007) as well as for a ZDI sample of stars with known activity cycle period. The inactive and active branches (marked as dashed lines) are labeled. One can see that there are different magnetic field topologies along each branch, with inactive branch stars all having dominantly poloidal fields whereas active branch stars are able to generate significant toroidal fields. The reason for this becomes clearer by looking at Figure 9b. It is known that solar-type stars with $Ro > 1$ display poloidal fields, while stars with $Ro < 1$ can generate strong toroidal fields (Donati & Landstreet 2009). Comparing Figure 9a and b, we see that, due to the shape of the $Ro = 1$ curve through period–mass space, inactive branch stars mostly have $Ro > 1$, explaining their poloidal fields. Conversely, active branch stars mostly have $Ro < 1$, explaining their toroidal fields. However, one should be cautious since for the shown ZDI sample the active and inactive branch stars are completely segregated by a rotational period of ~12 days. It is therefore not clear whether the different magnetic topologies on each branch are simply a result of their rotational period segregation or whether they are genuinely caused by some physical process such that surface fields should differ for stars on the two branches. This degeneracy can be broken by ZDI mapping of stars in the shaded region of Figure 9 where the two branches overlap in rotational period. If the hypothesis of genuinely different magnetic field configuration on the two branches is correct, stars with the same rotational period in the shaded region but on different branches should be found to have different field topologies. Further details are found in See et al. (2016).

## 5 | STELLAR MAGNETISM AND ITS IMPACT ON THE SURROUNDING ENVIRONMENT

In this section, we discuss stellar magnetism and winds, and the effect of stellar activity on exoplanet detection and the circumstellar environment.

### 5.1 | Stellar magnetic field inference, activity noise, and exoplanet searches

The strength and geometry of surface magnetic fields can nowadays be inferred for solar-type stars (with an increasing

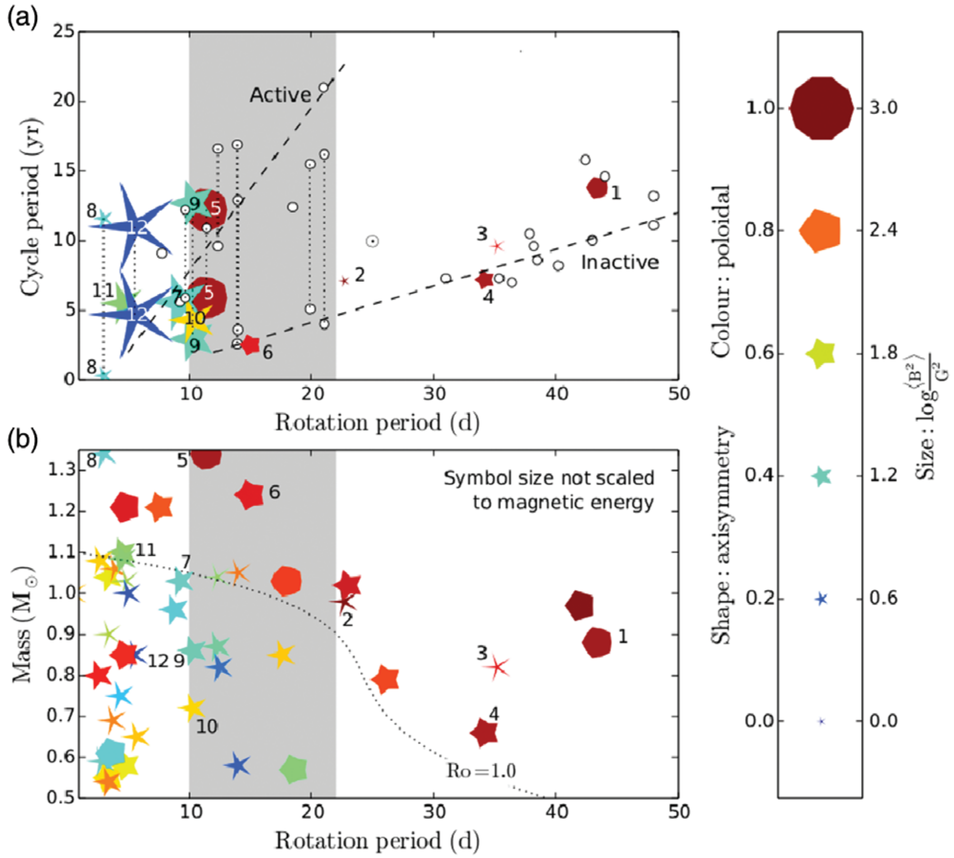


**FIGURE 9** (a) Period of the activity cycle versus period of rotation for the Böhm-Vitense (2007) sample, and for a sample of stars that have ZDI maps as well as chromospherically determined activity cycle period. (b) Mass versus rotational period for the sample studied by See et al. (2015). In both panels, the ZDI stars are plotted according to their magnetic properties. Red/blue symbols indicate poloidal/toroidal fields, and polygon/star shapes indicate axisymmetric/non-axisymmetric fields. In panel (a), symbol size corresponds to magnetic field energy

number of detections also in those older than ~2 Gyr) with the use of spectropolarimetry (e.g., Marsden 2016). Large-scale surface magnetic fields can also be mapped using ZDI. The extrapolation into the corona of radial field lines from the maps is then used to produce MHD models for the modeling of the stellar wind in a given star (and, thus, of the evolution and habitability of possible exoplanets). Jardine et al. (2016, 2017) find that, despite their relatively low spatial resolution, stellar ZDI magnetograms are able to recover well (within 5% for a typical stellar surface resolution of 20–30°) the average wind speeds of Sun-like stars (and predicted mass-loss rates compare well with those determined from fully 3D MHD wind models), while other wind parameters such as X-ray emission and rotational modulation are affected by smaller spatial-scale modes (contributed by structures such as, e.g., spots). All of these techniques reveal key details about the solar–stellar connection, with observations at multiple epochs showing simple years-long cyclic magnetic activity and polarity reversal, but also cases of complex variability and so far no apparent polarity switch. While the mean strength of the detected fields and the share of toroidal field tend to decrease with increasing age and rotational period, as expected, with older/slower stars having weaker fields of predominantly poloidal component, some objects do not fit the trend with rotational rate, which may be due to possible peculiar magnetic field geometry. Interestingly, for stars with Sun-like atmospheric parameters and an age close to that of the Sun at the time when life could have started on Earth, the outward extrapolation of magnetic fields seems to predict strong winds, with a mass-loss rate up to tens of times the current solar value.

Magnetic activity in solar-type stars can have an important influence on hosted planets. For example, most stars in the Milky Way are M dwarfs. These are often quite fast rotators, thus their surface magnetic flux can be expected to be considerable (in the case of fully convective M dwarfs, as recently shown by Shulyak et al. 2017, even above the so-far-presumed saturation limit of around 4 kG), with strong stellar flares and winds making the surrounding environment harsh. Moreover, they are less massive and less luminous than the current Sun, therefore a classically defined habitable zone exists only close to them. Planets in this zone around an M dwarf are thus likely to experience high fluxes of DNA-damaging radiation in the form of X-ray and extreme ultraviolet light, although slower rotation as their age increases might alleviate the detrimental effects on planetary atmospheres and habitability. The proximity to their host star of habitable planets around M dwarfs also increases the possibility of tidal locking, with unevenly heated planetary sides being a likely consequence.

The contribution of stellar magnetism to "stellar noise" affecting exoplanet searches has recently started to be explored in detail. For example, Haywood et al. (2016) recently studied disk-averaged solar radial-velocity variability, finding that the suppression of convective blueshift in facular regions of the Sun gives the dominant contribution to its activity-induced radial-velocity variations. Using such "Sun-as-a-star" observations of distortions in the spectral line profiles, one can hope to derive proxies to correct the radial velocities of other stars. Spot-induced jitter has recently been studied in M dwarfs by Barnes et al. (2016a, 2016b), who have found that intensive monitoring on time scales of days to weeks will be crucial to improve planet detection by modeling and mitigating activity-induced radial-velocity variations. Aigrain et al. (2016) pointed out that activity-induced stellar brightness variations due to spots can be modeled jointly with instrumental/pointing systematics for high-precision planetary transit studies and that simultaneous radial-velocity measurements can be used to constrain the contribution of faculae (to which photometry is mostly insensitive). In the case of studies at short wavelengths (high energies), where planetary transits are deeper but stellar magnetism noise is stronger, Llama et al. (2016) argue that simultaneous optical observations may be useful to remove activity signatures.

## 5.2 | Simulating the environment around planet-hosting stars

The discovery of the first extrasolar planet around a main sequence star by Mayor & Queloz (1995) sparked general interest in understanding the physical conditions around stars different from the Sun. One natural path to address this issue is to perform analogies with the solar system and to evaluate their range of applicability for describing other stellar systems. The characteristics and evolution of the solar magnetic field have been identified as the fundamental drivers of the physical conditions of the environment surrounding our host star (e.g., coronal properties, high-energy emission, solar wind, heliospheric structure, etc.). Given that the Sun is relatively inactive, it is fundamental to understand these magnetism–environment connections for stars with higher magnetic activity levels, because they can be expected to influence their circumstellar environment even more dramatically. This is nowadays possible with the aid of a combined methodology involving advanced observational techniques and sophisticated numerical simulations.

The observational component involves analysis of spectropolarimetric time series. Additionally, the ZDI technique (Brown et al. 1991; Donati & Brown 1997; Hussain et al. 2009; Kochukhov & Wade 2010; Piskunov & Kochukhov 2002; Semel 1989) is employed. A map of the surface large-scale magnetic field distribution is thus generated (e.g., Alvarado-Gómez et al. 2015; Hussain et al. 2016). Once the magnetic field topology is recovered, it can be incorporated

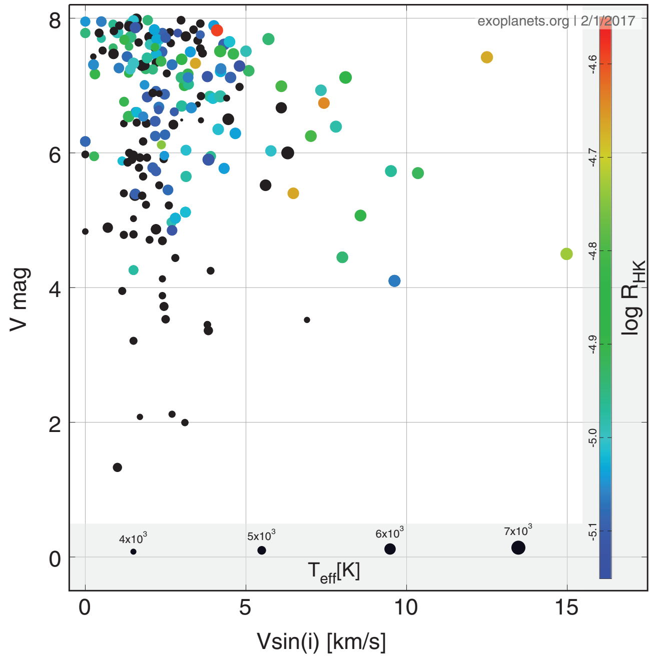


**FIGURE 10** Initial exploration for potential systems to be characterized with ZDI (adapted from http://exoplanets.org)

into a state-of-the-art numerical code used for space weather modeling and forecast in the solar system (e.g., the Space Weather Modelling Framework,[1] Tóth et al. 2005, 2012). In this way, a consistent data-driven characterization of the environment of each system can be obtained. To understand the capabilities and limitations of this modeling approach, solar and stellar simulations are systematically compared with each other and against observational data. This reveals that the procedure can properly recover the overall coronal and stellar wind conditions (reproducing successfully previous observational trends), up to magnetic activity levels of the order of ~100 times larger than the Sun in X-rays (see Alvarado-Gómez et al. 2016a, 2016b).

A way forward in this investigation is the expansion of the characterized sample to cover a broader range of stellar parameters, evolutionary stages, and activity levels. International collaborations, such as Bcool,[2] MaPP,[3] MaTYSSE,[4] and TOUPIES,[5] are currently increasing the database of spectropolarimetric observations and ZDI reconstructions.

In the case of planet-hosting stars, the number of systems with ZDI large-scale magnetic field reconstructions is still relatively small (see Fares 2014; Fares et al. 2013), but it has been slowly increasing in the last few years. This situation can be improved with additional ZDI observing campaigns of exoplanet hosts. Figure 10 shows an initial exploration in http://exoplanets.org for potential systems to

[1]Developed at The University of Michigan Center for Space Environment Modeling (CSEM) and made available through the NASA Community Coordinated Modeling Center (CCMC).
[2] http://bcool.ast.obs-mip.fr/Bcool/Bcool___cool_magnetic_stars.html
[3] http://lamwws.oamp.fr/magics/mapp/FrontPage
[4] https://matysse.irap.omp.eu/doku.php?id$=$start
[5] http://ipag.osug.fr/Anr_Toupies/spip.php?rubrique2

be studied with ZDI, taking into account the limitations of the technique with current instrumentation. Relatively bright objects ($V_{\rm mag} \leq 8.0$) with moderate magnetic activity ($\log R_{\rm HK} > -5.0$; *cyan* to *red* symbols in Figure 10) are required to robustly detect and map the surface large-scale magnetic field with current instrumentation. While a significant number of planet-hosting stars lack chromospheric activity information (*black* symbols in Figure 10), the statistics of the BCool snapshot survey presented by Marsden et al. (2014) indicate definitive magnetic field detections in ~25–50% of the stars within this range of rotational velocities ($v \sin(i) \leq 6.0\,{\rm km\,s^{-1}}$) using circular spectropolarimetry, thus ZDI reconstruction should be possible for them: the better the spatial resolution of the recovered ZDI map, the larger the $v \sin(i)$ of the star. This simple exploration shows that, with the aid of current facilities, such ZDI-driven methodology could be applied to a considerable number of systems, including more than ~100 planet-hosting stars (Figure 10). Future instrumentation with similar capabilities, such as SPiRou,[6] Neo-Narval,[7] and CRIRES+,[8] will significantly increase this working sample, maximizing the impact of this methodology on the research fields of stellar magnetism and exoplanet characterization.

## 6 | CONCLUDING REMARKS AND FUTURE OUTLOOK

Magnetic fields strongly influence the evolution of stars from their formation to the end of their life cycle. We reviewed some of the recent progress and developments in the study of the variability of magnetic activity in solar-type stars. We highlighted crucial unsolved questions regarding the generation and interaction of convection, magnetic fields, differential rotation, and meridional circulation. In particular, we discussed how better understanding of solar variability, of the dynamo process, and of flux emergence phenomena will be key to advancing studies of the solar–stellar connection, of the variability of magnetic activity throughout stellar evolution (in particular, of the age–rotation–activity relationship), and of the impact of stellar magnetism on planetary environment and habitability.

With respect to observations, data from new surveys, for example *Kepler*'s second mission (*K2*, Howell et al. 2014), will greatly contribute to clarifying the physics that underlies the separation of stars into activity branches, and thus to more precisely relate stellar mass (color) and age to stellar rotation and activity. The loss of angular momentum is an important physical phenomenon acting throughout stellar evolution. Through future improvements in the accuracy of maps of stellar magnetic fields and of stellar wind modeling, it should be possible to reveal in detail how the strength of rotational spin-down depends on the geometrical configuration of stellar magnetic fields. The new data will also allow us to test the use of gyrochronology beyond 1 Gyr using calibration with old field stars of known asteroseismic ages. The connection between rotational evolution and magnetic fields should also be explored using more observations of very young stars and through photometry measurements. New observations of M dwarfs of different masses and ages (e.g., using the CARMENES instrument, see Quirrenbach et al. 2016) will play a key role in our understanding the similarities and differences in magnetic activity between Sun-like stars and fully convective ones.

It is highly desirable to make a significant step forward in our understanding of the principles driving stellar dynamos throughout stellar evolution. To this purpose, improvements are necessary from both theoretical and observational perspectives. Within the solar dynamo modeling community in particular, there is a lively debate about the importance of the tachocline. A clear consensus is still lacking, with some simulations finding that the radial shear in the tachocline holds great significance (but with difficulties in some cases to trap the radial shear across the convective–radiative boundary, see e.g., Brun et al. 2015), whereas in many mean-field models the radial shear does not play any role. We presented the latest developments in modeling the Babcock–Leighton mechanism and highlighted the importance of the role played by the meridional circulation (which remains largely unconstrained by observations and therefore is the weakest point from a dynamo model point of view). Within this context, only helioseismic and asteroseismic observations can help solve the issue. In particular, they can provide key advances in terms of (a) knowledge of the depth of penetration of meridional circulation below the base of the convection zone, and (b) knowledge of the depth at which the latitudinal component of meridional circulation reverses to equatorward.

While helioseismology and asteroseismology are the only tools to probe solar and stellar interiors, the wealth of information coming from statistical studies of the properties of stellar magnetic activity throughout evolution offers a different perspective on the dynamo mechanism. They will help us to distinguish between the large-scale dynamo initiated since the early life of the stars and the one emerging only at specific stages of the star (e.g., see the study by Privitera et al. 2016 on the dynamo mechanism in red giants).

Finally, the retrieval of detailed information about the effect of stellar magnetic activity on the surrounding environment and on the habitability and detectability of planets is an obvious priority. Crucial new hints on the characteristics of both representative and peculiar planetary systems are being constantly added. For example, the discovery of the planetary system TRAPPIST-1 (Gillon et al. 2017) has opened up new frontiers. This planet-hosting system is remarkable for several reasons. The star at the system's center (an M

[6] http://spirou.irap.omp.eu/
[7] http://www.tbl.obs-mip.fr/INSTRUMENTATION2/neonarval
[8] http://www.eso.org/sci/facilities/develop/instruments/crires_up.html∖#par&uscore;title

dwarf) is exceptionally cool, emitting mainly in the infrared. *XMM-Newton* data revealed that, despite its much lower photospheric luminosity compared to our own (much larger) host star, TRAPPIST-1 emits X-rays at a level comparable to that of the Sun (Wheatley et al. 2017). All seven of its planets are Earth-sized and orbit closer (thus feeling strong irradiation) than the planet Mercury does to the Sun. Moreover, the compact configuration of the TRAPPIST-1 system can be used as a testing ground for our current knowledge about planet formation. For example, it could be that the seven exoplanets formed further from their star and moved inward over time, eventually coming to their current arrangement. Remotely studying the chemical compositions of their atmospheres will also contribute to a better insight into terrestrial worlds beyond our Solar system.

## ACKNOWLEDGMENTS

D.F. and R.S. thank the organizers of the 19th Cambridge Workshop on Cool Stars, Stellar Systems, and the Sun ("Cool Stars 19") for giving us the opportunity of holding a splinter session on the topic of the "Variability of Solar/Stellar Magnetic Activity". We thank all participants who took part in it for contributing to its success with their interest and with their inspiring questions and answers. The main scientific issues that arose and were addressed during the two afternoons of the splinter session form the core of this article. D.F. is grateful to Robert Cameron for useful discussion and suggestions. R.B. would like to thank her PhD supervisor, Katja Poppenhaeger, for her continued support.

D.F. acknowledges the support by the German Federal Ministry for Education and Research through the "Role Of the MIddle atmosphere in Climate" (ROMIC) project. The National Solar Observatory is operated by the Association of Universities for Research in Astronomy, Inc. (AURA) under cooperative agreement with the National Science Foundation. Funding for the Stellar Astrophysics Centre is provided by The Danish National Research Foundation (Grant DNRF106). K.O. acknowledges support from the Hungarian National Research, Development and Innovation Office grant OTKA K-109276. J.D.A.G. was supported by *Chandra* grants AR4-15000X and GO5-16021X. R.B. gratefully acknowledges the Royal Astronomical Society for the grant awarded that helped fund her travel to the 19th Cool Stars conference. V.S. acknowledges the support of a Science & Technology Facilities Council (STFC) postdoctoral fellowship.

## REFERENCES


Adibekyan, V., Delgado-Mena, E., Feltzing, S., et al. 2017, *AN*, *338*, 442.
Aigrain, S., Angus, R., Barstow, J., et al. 2016, 19th Cambridge Workshop on Cool Stars, Stellar Systems, and the Sun (CS19), 12.
Alvarado-Gómez, J. D., Hussain, G. A. J., Grunhut, J., et al. 2015, *A&A*, *582*, A38.
Alvarado-Gómez, J. D., Hussain, G. A. J., Cohen, O., et al. 2016a, *A&A*, *588*, A28.
Alvarado-Gómez, J. D., Hussain, G. A. J., Cohen, O., et al. 2016b, *A&A*, *594*, A95.
Asplund, M., Grevesse, N., Sauval, A. J., & Scott, P. 2009, *ARA&A*, *47*, 481.
Augustson, K. C., Brown, B. P., Brun, A. S., et al. 2012, *ApJ*, *756*, 169.
Augustson, K. C., Brun, A. S., & Toomre, J. 2013, *ApJ*, *777*, 153.
Baglin, A., Auvergne, M., Boisnard, L., et al. 2006, COSPAR, Plenary Meeting, 36th COSPAR Scientific Assembly, Vol. 36, 3749.
Baliunas, S. L., & Vaughan, A. H. 1985, *ARA&A*, *23*, 379.
Baliunas, S. L., Donahue, R. A., Soon, W. H., et al. 1995, *ApJ*, *438*, 269.
Ball, W. H., Beeck, B., Cameron, R. H., & Gizon, L. 2016, *A&A*, *592*, 159.
Ballot, J., Brun, A. S., & Turck-Chièze, S. 2007, *ApJ*, *669*, 1190.
Barnes, S. A. 2007, *ApJ*, *669*, 1167.
Barnes, S. A. 2010, *ApJ*, *722*, 222.
Barnes, J., Haswell, C., Jenkins, J., et al. 2016a, 19th Cambridge Workshop on Cool Stars, Stellar Systems, and the Sun (CS19), 10.
Barnes, S. A., Weingrill, J., Fritzewski, D., et al. 2016b, *ApJ*, *823*, 16.
Basri, G. 2016, 19th Cambridge Workshop on Cool Stars, Stellar Systems, and the Sun (CS19), 17.
Beeck, B., Schüssler, M., Cameron, R. H., & Reiners, A. 2015, *A&A*, *581*, A43.
Berdyugina, S. V., Pelt, J., & Tuominen, I. 2002, *A&A*, *394*, 505.
Bessell, M. S., Castelli, F., & Plez, B. 1998, *A&A*, *333*, 231.
Böhm-Vitense, E. 2007, *ApJ*, *657*, 486.
Booth, R., & Poppenhaeger, K. 2016, 19th Cambridge Workshop on Cool Stars, Stellar Systems, and the Sun (CS19), 23.
Booth, R. S., Poppenhaeger, K., Watson, C. A., et al. 2017, *MNRAS*, *471*, 1012.
Borucki, W. J., Koch, D., Basri, G., et al. 2010, *Science*, *327*, 977.
Brandenburg, A., Saar, S. H., & Turpin, C. R. 1998, *ApJ*, *498*, L51.
Brandenburg, A. 2005, *ApJ*, *625*, 539.
Brandenburg, A., Kleeorin, N., & Rogachevskii, I. 2013, *ApJ*, *776*, L23.
Brown, S. F., Donati, J.-F., Rees, D. E., & Semel, M. 1991, *A&A*, *250*, 463.
Brown, B. P., Browning, M. K., Brun, A. S., et al. 2008, *ApJ*, *689*, 1354–1372.
Brown, B. P., Miesch, M. S., Browning, M. K., et al. 2011, *ApJ*, *731*, 69.
Brun, A. S., Browning, M. K., Dikpati, M., et al. 2015, *Space Sci. Rev.*, *196*, 101.
Cameron, R., & Schüssler, M. 2007, *ApJ*, *659*, 801.
Cayrel de Strobel, G., Knowles, N., Hernandez, G., & Bentolila, C. 1981, *A&A*, *94*, 1.
Chaplin, W. J., Kjeldsen, H., & Christensen-Dalsgaard, J. 2011a, *Science*, *332*, 213.
Chaplin, W. J., Bedding, T. R., Bonanno, A., et al. 2011b, *ApJ*, *732*, L5.
Chaplin, W. J., Basu, S., Huber, D., et al. 2014, *ApJS*, *210*, 1.
Charbonneau, P. 2005, *Living Rev. Solar Phys.*, *2*, 2.
Cheung, M. C. M., & Isobe, H. 2014, *Living Rev. Solar Phys.*, *11*, 3.
Chiavassa, A., Collet, R., Casagrande, L., & Asplund, M. 2010, *A&A*, *524*, 93.
Christensen, U. R., & Aubert, J. 2006, *Geophys. J. Int.*, *166*, 97.
Cole, E., Käpylä, P. J., Mantere, M. J., & Brandenburg, A. 2014, *ApJ*, *780*, 22.
Collet, R., Asplund, M., & Trampedach, R. 2007, *A&A*, *469*, 687.
Collet, R., Criscuoli, S., Ermolli, I., et al. 2016, arXiv:1612.02348.
Cranmer, S. R., & Saar, S. H. 2011, *ApJ*, *741*, 54.
Criscuoli, S., & Uitenbroek, H. 2014, *ApJ*, *788*, 151.
Dasi-Espuig, M., Jiang, J., Krivova, N. A., & Solanki, S. K. 2014, *A&A*, *570*, A23.
Dasi-Espuig, M., Jiang, J., Krivova, N. A., et al. 2016, *A&A*, *590*, A63.
De Pontieu, B., Title, A. M., Lemen, J. R., et al. 2014, *Sol. Phys.*, *289*, 2733.
De Silva, G. M., Freeman, K. C., Bland-Hawthorn, J., et al. 2015, *MNRAS*, *449*, 2604.
Dikpati, M., & Charbonneau, P. 1999, *ApJ*, *518*, 508.
Dikpati, M., & Anderson, J. L. 2014, AGU Fall Meeting Abstracts.
Do Cao, O., & Brun, A. S. 2011, *AN*, *332*, 907.
Domingo, V., Ermolli, I., Fox, P., et al. 2009, *SSRv*, *145*, 337.
Donati, J.-F., & Brown, S. F. 1997, *A&A*, *326*, 1135.
Donati, J.-F., & Landstreet, J. D. 2009, *ARA&A*, *47*, 333.
Dorren, J. D., & Guinan, E. F. 1994, *ApJ*, *428*, 805.
Durney, B. R., De Young, D. S., & Roxburgh, I. W. 1993, *Sol. Phys.*, *145*, 207.
Eberhard, G., & Schwarzschild, K. 1913, *ApJ*, *38*, 292.
Egeland, R., Metcalfe, T. S., Hall, J. C., & Henry, G. W. 2015, *ApJ*, *812*, 12.
Ermolli, I., Matthes, K., Dudok de Wit, T., et al. 2013, *ACP*, *13*, 3945.
Ermolli, I., Shibasaki, K., Tlatov, A., & van Driel-Gesztelyi, L. 2014, *SSRv*, *186*, 105.
Fabbian, D., Khomenko, E., Moreno-Insertis, F., & Nordlund, Å. 2010, *ApJ*, *724*, 1536.
Fabbian, D., Moreno-Insertis, F., Khomenko, E., & Nordlund, Å. 2012, *A&A*, *548*, A35.
Fabbian, D., & Moreno-Insertis, F. 2015, *ApJ*, *802*, 96.
Fan, Y. 2004, *Living Rev. Solar Phys.*, *1*, 1.
Fan, Y., & Fang, F. 2014, *ApJ*, *789*, 35.
Fares, R., Moutou, C., Donati, J.-F., et al. 2013, *MNRAS*, *435*, 1451.
Fares, R. 2014, Magnetic Fields throughout Stellar Evolution, 302, 180.

Featherstone, N. A., & Miesch, M. S. 2015, *ApJ*, *804*, 67.
Fletcher, S. T., Broomhall, A.-M., Salabert, D., et al. 2010, *ApJ*, *718*, L19.
Folsom, C. P., Petit, P., Bouvier, J., et al. 2016, *MNRAS*, *457*, 580.
Fröhlich, C. 2003, Solar Variability as an Input to the Earth's Environment, ESA-SP 535, 183.
García, R. A., Mathur, S., Salabert, D., et al. 2010, *Science*, *329*, 1032.
García, R. A., Hekker, S., Stello, D., et al. 2011, *MNRAS*, *414*, L6.
García, R. A., Ceillier, T., Salabert, D., et al. 2014, *A&A*, *572*, A34.
Garraffo, C., Drake, J. J., & Cohen, O. 2015, *ApJ*, *813*, 40.
Gastine, T., Yadav, R. K., Morin, J., et al. 2014, *MNRAS*, *438*, L76.
Giampapa, M. 2016, 19th Cambridge Workshop on Cool Stars, Stellar Systems, and the Sun (CS19), 1.
Gillon, M., Trudy, A. M. J., Demory, B. O., et al. 2017, *Nature*, *542*, 456–460.
Gilman, P. A., & Miller, J. 1981, *ApJS*, *46*, 211.
Gizon, L., Birch, A. C., & Spruit, H. C. 2010, *ARA&A*, *48*, 289.
Gleissberg, W. 1939, *The Observatory*, *62*, 158.
Greenhouse, M. A. 2016, *Proc. SPIE*, *9904*, 990406.
Güdel, M. 2007, *Living Rev. Solar Phys.*, *4*, 3.
Guerrero, G., & de Gouveia Dal Pino, E. M. 2008, *A&A*, *485*, 267.
Guerrero, G., Smolarkiewicz, P. K., de Gouveia Dal Pino, E. M., et al. 2016, *ApJ*, *819*, 104.
Hackman, T., Mantere, M. J., Jetsu, L., et al. 2011, *AN*, *332*, 859.
Hall, J. C. 2008, *Living Rev. Solar Phys.*, *5*, 2.
Harvey, J. W., Hudson, H. S., Noyes, R. W., & Zirker, J. B. 1985, *Science*, *230*, 660.
Haywood, R. D., Collier Cameron, A., Dumusque, X., et al. 2016, 19th Cambridge Workshop on Cool Stars, Stellar Systems, and the Sun (CS19), 47.
Hazra, S., Passos, D., & Nandy, D. 2014, *ApJ*, *789*, 5.
Hickey, J. R., Stowe, L. L., Jacobowitz, H., et al. 1980, *Science*, *208*, 281.
Holzwarth, V., & Schüssler, M. 2001, *A&A*, *377*, 251.
Holzwarth, V., Mackay, D. H., & Jardine, M. 2006, *MNRAS*, *369*, 1703.
Howell, S. B., Sobeck, C., Haas, M., et al. 2014, *PASP*, *126*, 398.
Hung, C. P., Jouve, L., Brun, A.-S., Fournier, A., & Talagrand, O. 2015, EGU General Assembly Conference Abstracts, 17, 10832.
Hussain, G. A. J., Collier Cameron, A., Jardine, M. M., et al. 2009, *MNRAS*, *398*, 189.
Hussain, G. A. J., Alvarado-Gómez, J. D., Grunhut, J., et al. 2016, *A&A*, *585*, A77.
Inceoglu, F., Simoniello, R., Knudsen, M. F., et al. 2016, *Sol. Phys.*, *291*, 303.
Jackson, A. P., Davis, T. A., & Wheatly, P. J. 2012, *MNRAS*, *422*, 2024.
de Jager, C., Akasofu, S.-I., Duhau, S., et al. 2016, *Space Sci. Rev.*, *201*, 109.
Jardine, M., See, V., & Vidotto, A. 2016, 19th Cambridge Workshop on Cool Stars, Stellar Systems, and the Sun (CS19), 15.
Jardine, M., Vidotto, A. A., & See, V. 2017, *MNRAS*, *465*, L25.
Jiang, J., Hathaway, D. H., Cameron, R. H., et al. 2014, *Space Sci. Rev.*, *186*, 491.
Jiménez, A., García, R. A., Pérez Hernández, F., & Mathur, S. 2015, *A&A*, *583*, A74.
de Jong, R. S., Barden, S., Bellido-Tirado, O., et al. 2014, *Proc. SPIE*, *9147*, 91470M.
Jouve, L., & Brun, A. S. 2007, *A&A*, *474*, 239.
Jouve, L., Brown, B. P., & Brun, A. S. 2010, *A&A*, *509*, A32.
Jouve, L., Brun, A. S., & Aulanier, G. 2013, *ApJ*, *762*, 4.
Käpylä, P. J., Mantere, M. J., Cole, E., et al. 2013, *ApJ*, *778*, 41.
Kawaler, S. D. 1988, *ApJ*, *333*, 236.
Kitchatinov, L. L., & Rüdiger, G. 2004, *AN*, *325*, 496.
Knaack, R., Fligge, M., Solanki, S. K., & Unruh, Y. C. 2001, *A&A*, *376*, 1080.
Knudsen, M. F., Riisager, P., Jacobsen, B. H., et al. 2009, *Geophys. Res. Lett.*, *36*, L16701.
Kochukhov, O., & Wade, G. A. 2010, *A&A*, *513*, A13.
Kochukhov, O., Petit, P., Strassmeier, K. G., et al. 2017, *AN*, *338*, 428.
Kolláth, Z., & Oláh, K. 2009, *A&A*, *501*, 695.
Kopp, G. 2016, *JSWSC*, *6*, 30.
Kopp, G., Krivova, N., Wu, C. J., & Lean, J. 2016, *Sol. Phys.*, *291*, 2951.
Kosugi, T., Matsuzaki, K., Sakao, T., et al. 2007, *Sol. Phys.*, *243*, 3.
Kővári, Z., & Oláh, K. 2014, *Space Sci. Rev.*, *186*, 457.
Kővári, Z., Kriskovics, L., Künstler, A., et al. 2015, *A&A*, *573*, A98.
Kraft, R. P. 1967, *ApJ*, *150*, 551.
Krause, F., & Raedler, K. H. 1980, Mean-field magnetohydrodynamics and dynamo theory. Pergamon Press (Oxford).
Lehtinen, J., Jetsu, L., Hackman, T., et al. 2016, *A&A*, *588*, 38L.
Lindborg, M., Korpi, M. J., Hackman, T., et al. 2011, *A&A*, *526*, 44L.
Livingston, W. C. 1982, *Nature*, *297*, 208.
Livingston, W., & Holweger, H. 1982, *ApJ*, *252*, 375.
Livingston, W., Milkey, R., & Slaughter, C. 1977, *ApJ*, *211*, 281.
Llama, J., Shkolnik, E., Cameron, A., & Jardine, M. 2016, 19th Cambridge Workshop on Cool Stars, Stellar Systems, and the Sun (CS19), 13.
Lockwood, G. W., Skiff, B. A., Baliunas, S. L., & Radick, R. R. 1992, *Nature*, *360*, 653.
Lockwood, M., & Owens, M. J. 2014, *ApJ*, *781*, L7.
Lockwood, M., Stamper, R., & Wild, M. N. 1999, *Nature*, *399*, 437.
Lockwood, G. W., Skiff, B. A., Henry, G. W., et al. 2007, *ApJS*, *171*, 260.
MacGregor, K. B., & Charbonneau, P. 1997, *ApJ*, *486*, 484.
Marchenko, S. V., & DeLand, M. T. 2014, *ApJ*, *789*, 117.
Marsden, S. C., Petit, P., Jeffers, S. V., et al. 2014, *MNRAS*, *444*, 3517.
Marsden, S. 2016, 19th Cambridge Workshop on Cool Stars, Stellar Systems, and the Sun (CS19), 11.
Martínez-Sykora, J., Hansteen, V., & Carlsson, M. 2008, *ApJ*, *679*, 871–888.
Marvin, C., Reiners, A., Anglada-Escudé, G., Jeffers, S., & Boro-Saikia, S. 2016, 19th Cambridge Workshop on Cool Stars, Stellar Systems, and the Sun (CS19), 8.
Mathur, S., Hekker, S., Trampedach, R., et al. 2011, *ApJ*, *741*, 119.
Mathur, S., García, R. A., Ballot, J., et al. 2014, *A&A*, *562*, 124.
Mathur, S., Huber, D., Batalha, N. M., et al. 2017, *ApJS*, *229*, 30.
Mayor, M., & Queloz, D. 1995, *Nature*, *378*, 355.
McQuillan, A., Mazeh, T., & Aigrain, S. 2014, *ApJS*, *211*, 24.
Meibom, S., Barnes, S. A., Latham, D. W., et al. 2011, *ApJ*, *733*, L9.
Metcalfe, T. S., Creevey, O. L., Dogan, G., et al. 2014, *ApJS*, *214*, 27.
Metcalfe, T. S., Egeland, R., & van Saders, J. 2016, *ApJ*, *826*, L2.
Mignard, F. 2005, Astrometry in the Age of the Next Generation of Large Telescopes, 338, 15.
Mitchell, W. E. Jr., & Livingston, W. C. 1991, *ApJ*, *372*, 336.
Moffatt, H. K. 1978, Magnetic field generation in electrically conducting fluids. Cambridge University Press (Cambridge, England), 353 p.
Moore, C. S., Uitenbroek, H., Rempel, M., et al. 2016, *ApJ*, *799*, 150.
Morin, J., Donati, J.-F., Petit, P., et al. 2010, *MNRAS*, *407*, 2269.
Mosser, B., Baudin, F., Lanza, A. F., et al. 2009a, *A&A*, *506*, 245.
Mosser, B., Michel, E., Appourchaux, T., et al. 2009b, *A&A*, *506*, 33.
Müller, D., Marsden, R. G., St. Cyr, O. C., & Gilbert, H. R. 2013, *Sol. Phys.*, *285*, 25.
do Nascimento, J.-D. Jr., García, R. A., Mathur, S., et al. 2014, *ApJ*, *790*, LL23.
Nelson, N. J., Brown, B. P., Brun, A. S., et al. 2013, *ApJ*, *762*, 73.
Nelson, N. J., Brown, B. P., Sacha Brun, A., et al. 2014, *Sol. Phys.*, *289*, 441.
Nordlund, Å., Stein, R. F., & Asplund, M. 2009, *Living Rev. Solar Phys.*, *6*, 2.
Oláh, K., Kolláth, Z., Granzer, T., et al. 2009, *A&A*, *501*, 703.
Oláh, K., Kővári, Z., Petrovay, K., et al. 2016, *A&A*, *590*, 1330.
Pallavicini, R., Golub, L., Rosner, R., et al. 1981, *ApJ*, *248*, 279.
Parker, E. N. 1955, *ApJ*, *122*, 293.
Parker, E. N. 1985, *Sol. Phys.*, *100*, 599.
Parker, E. N. 1993, *ApJ*, *408*, 707.
Pesnell, W. D., Thompson, B. J., & Chamberlin, P. C. 2012, *Sol. Phys.*, *275*, 3.
Petrovay, K. 2010, *Living Rev. Solar Phys.*, *7*, 6.
Piskunov, N., & Kochukhov, O. 2002, *A&A*, *381*, 736.
Pizzolato, N., Maggio, A., Micela, G., et al. 2003, *A&A*, *397*, 147.
Porto de Mello, G. F., & da Silva, L. 1997, *ApJ*, *482*, L89.
Privitera, G., Meynet, G., Eggenberger, P., et al. 2016, *A&A*, *593*, L15.
Quirrenbach, A., Amado, P. J., Caballero, J. A., et al. 2016, *Proc. SPIE*, *9908*, 990812.
Raedler, K.-H. 1986, *AN*, *307*, 89.
Rauer, H., Aerts, C., Cabrera, J., & Team, P. L. A. T. O. 2016, *AN*, *337*, 961.
Reiners, A., & Basri, G. 2009, *A&A*, *496*, 787.
Reiners, A., & Mohanty, S. 2012, *ApJ*, *746*, 43.
Reinhold, T., Reiners, A., & Basri, G. 2013, *A&A*, *560*, A4.
Ricker, G. R., Winn, J. N., Vanderspek, R., et al. 2015, *J. Astron. Telesc. Instrum. Syst.*, *1*, 014003.
Rüdiger, G., Kitchatinov, L. L., & Hollerbach, R. 2013, in: *Magnetic Processes in Astrophysics: Theory, Simulations, Experiments*, , eds. G. Rüdiger, L. L. Kitchatinov, & R. Hollerbach, Wiley-VCH, ISBN 978-3-527-41034-7.
Ruediger, G., & Brandenburg, A. 1995, *A&A*, *296*, 557.
Saar, S. H., & Baliunas, S. L. 1992, *The Solar Cycle*, *27*, 150.
Saar, S. H., & Brandenburg, A. 1999, *ApJ*, *524*, 295.
van Saders, J. L., Ceillier, T., Metcalfe, T. S., et al. 2016, *Nature*, *529*, 181.
Salabert, D., García, R. A., Beck, P. G., et al. 2016a, *A&A*, *596*, A31.
Salabert, D., Régulo, C., García, R. A., et al. 2016b, *A&A*, *589*, A118.

Schatten, K. H. 1993, *J. Geophys. Res.*, *98*, 18.
Schuessler, M., & Solanki, S. K. 1992, *A&A*, *264*, L13.
See, V., Jardine, M., Vidotto, A. A., et al. 2015, *MNRAS*, *453*, 4301.
See, V., Jardine, M., Vidotto, A. A., et al. 2016, *MNRAS*, *462*, 4442.
Seleznyov, A. D., Solanki, S. K., & Krivova, N. A. 2011, *A&A*, *532*, A108.
Semel, M. 1989, *A&A*, *225*, 456.
Shapiro, A. I., Solanki, S. K., Krivova, N. A., et al. 2014, *A&A*, *569*, A38.
Shapiro, A. I., Solanki, S. K., Krivova, N. A., et al. 2015, *A&A*, *581*, A116.
Shulyak, D., Reiners, A., Engeln, A., et al. 2017, *Nat. Astron.*, *1*, 0184.
Simoniello, R., Finsterle, W., García, R. A., et al. 2010, *A&A*, *516*, A30.
Simoniello, R., Jain, K., Tripathy, S. C., et al. 2013, *ApJ*, *765*, 100.
Simoniello, R., Tripathy, S. C., Jain, K., & Hill, F. 2016, *ApJ*, *828*, 41.
Skumanich, A. 1972, *ApJ*, *171*, 565.
Solanki, S. K., Schüssler, M., & Fligge, M. 2000, *Nature*, *408*, 445.
Solanki, S. K., Schüssler, M., & Fligge, M. 2002, *A&A*, *383*, 706.
Solanki, S. K., Krivova, N. A., & Haigh, J. D. 2013, *ARA&A*, *51*, 311.
Spiegel, E. A., & Weiss, N. O. 1980, *Nature*, *287*, 616.
Steenbeck, M., & Krause, F. 1969, *AN*, *291*, 49.
Stein, R. F., & Nordlund, Å. 2012, *ApJ*, *753*, L13.
Strassmeier, K. G., Rice, J. B., Wehlau, W. H., et al. 1991, *A&A*, *247*, 130.
Strassmeier, K. G., Boyd, L. J., Epand, D. H., & Granzer, T. 1997, *PASP*, *109*, 697.
Strassmeier, K. G., Granzer, T., Weber, M., et al. 2004, *AN*, *325*, 527.
Tóth, G., Sokolov, I. V., Gombosi, T. I., et al. 2005, *J. Geophys. Res. (Space Phys.)*, *110*, A12226.
Tóth, G., van der Holst, B., Sokolov, I. V., et al. 2012, *J. Comput. Phys.*, *231*, 870.
Trampedach, R., Aarslev, M. J., Houdek, G., et al. 2017, *MNRAS*, *466*, 43.
Tritschler, A., Rimmele, T.R., Berukoff, S., et al. 2016, *Astronomische Nachrichten*, *337*, 1064.
Uitenbroek, H., & Criscuoli, S. 2011, *ApJ*, *736*, 69.
Unruh, Y. C., Solanki, S. K., & Fligge, M. 1999, *A&A*, *345*, 635.
Upton, L., & Hathaway, D. H. 2014, *ApJ*, *780*, 5.
Usoskin, I. G. 2013, *Living Rev. Solar Phys.*, *10*, 1.
Usoskin, I. G., Arlt, R., Asvestari, E., et al. 2015, *A&A*, *581*, A95.
Usoskin, I. G. 2017, *Living Rev. Solar Phys.*, *14*, 3.
Vaughan, A. H., & Preston, G. W. 1980, *PASP*, *92*, 385.
Vecchio, A., & Carbone, V. 2009, *A&A*, *502*, 981.
Vida, K., Oláh, K., & Szabó, R. 2014, *MNRAS*, *441*, 2744.
Vidotto, A. A., Gregory, S. G., Jardine, M., et al. 2014, *MNRAS*, *441*, 2361.
Vidotto, A. A., Donati, J. F., Jardine, M., et al. 2016, *MNRAS*, *455*, L52.
Vogt, S. S., & Penrod, G. D. 1983, *PASP*, *95*, 565.
Walkowicz, L. M., & Basri, G. S. 2013, *MNRAS*, *436*, 1883.
Wang, Y.-M., & Sheeley, N. R. Jr. 1991, *ApJ*, *375*, 761.
Weber, M. A., & Browning, M. K. 2016, *ApJ*, *827*, 95.
West, A. A., Hawley, S. L., Bochanski, J. J., et al. 2008, *AJ*, *135*, 785.
Wheatley, P. J., Louden, T., Bourrier, V., et al. 2017, *MNRAS*, *465*, L74.
Willson, R. C., & Hudson, H. S. 1988, *Nature*, *332*, 810.
Wilson, O. C. 1963, *ApJ*, *138*, 832.
Wilson, O. C. 1968, *ApJ*, *153*, 221.
Wilson, O. C. 1978, *ApJ*, *226*, 379.
Wright, N. J., Drake, J. J., Mamajek, E. E., & Henry, G. W. 2011, *ApJ*, *743*, 48.
Wright, N. J., & Drake, J. J. 2016, *Nature*, *535*, 526.
Yadav, R. K., Christensen, U. R., Morin, J., et al. 2015, *ApJ*, *813*, L31.
Yelles Chaouche, L., Cheung, M. C. M., Solanki, S. K., et al. 2009, *A&A*, *507*, L53.
Yeo, K. L., Shapiro, A. I., Krivova, N. A., & Solanki, S. K. 2016, Coimbra Solar Physics Meeting: Ground-based Solar Observations in the Space Instrumentation Era, 504, 273.
Zaqarashvili, T. V., Carbonell, M., Oliver, R., & Ballester, J. L. 2010, *ApJ*, *724*, L95.
Zasowski, G., Johnson, J. A., Frinchaboy, P. M., et al. 2013, *AJ*, *146*, 81.

**How to cite this article:** Fabbian D, Simoniello R, Collet R, et al. The variability of magnetic activity in solar-type stars. *Astron. Nachr./AN.* 2017;338:753–772. https://doi.org/10.1002/asna.201713403.